MASTER THESIS

Bacterial interactions across a porous membrane

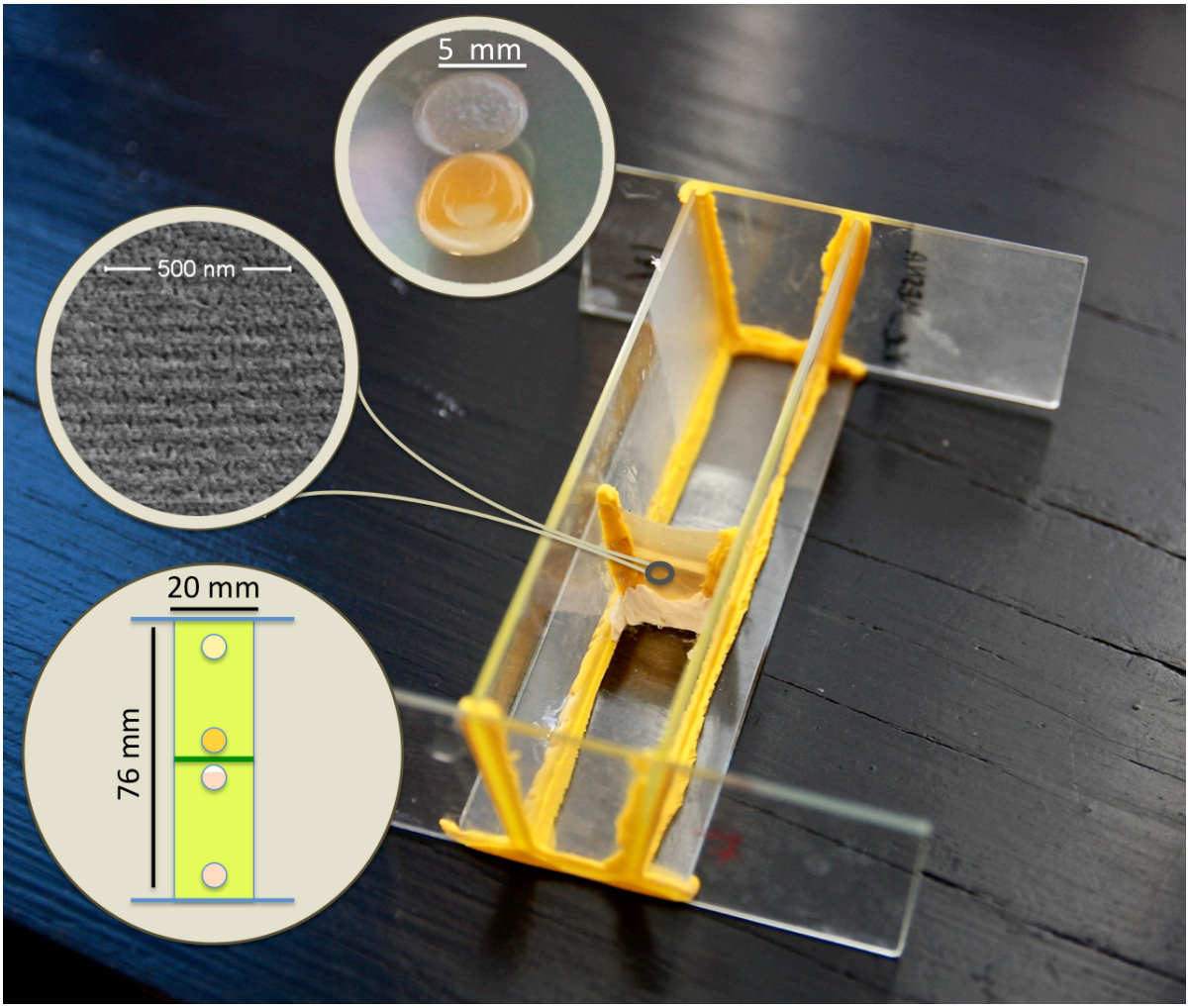

Malin Alsved & Karin Hjerpe
Nano technology engineering, LTH

LUND UNIVERSITY

MASTER THESIS

Bacterial interactions across a porous membrane

Malin Alsved & Karin Hjerpe

Supervised by:

Sokol Ndoni, Nanotech, DTU
Charlotte Frydenlund Michelsen and Claus Sternberg, System biology, DTU
Johan Svensson Bonde, Pure and Applied Biochemistry, LTH

Examinator:

Leif Bülow

A thesis submitted in fulfillment of the requirements for the degree of Master of Science in Engineering in the

Division of Pure and Applied Biochemistry
Lund University

Abstract

Deepening our knowledge about bacterial infections is of high priority in the work against antimicrobial resistance. Many infections are as well polymicrobial, and the different bacterial species are able to affect each other by cell-cell communication. This is a phenomenon that in several cases is known to enhance the virulence and the severity of the infection. Therefore, new approaches to study bacterial interactions are needed.

In this project we have designed a bacterial growth chamber with a porous membrane as a separating wall between two bacterial species. This gave us the ability to discriminate what molecules that can be exchanged between the bacterial cultures by choosing the membrane properties. The setup allows the two bacterial cultures to be spatially separated, yet chemically connected via diffusion through the growth medium and the porous membrane. Two different kinds of hydrophilic membranes were chosen for investigation of their performance as filters in this membrane setup for bacterial growth: a block copolymer based membrane with a pore size of 10 nm and commercially available Millipore membranes with two pore sizes of 220 and 450 nm respectively.

The studied bacterial interaction is between *Pseudomonas aeruginosa* and *Staphylococcus aureus*, two commonly found bacterial species in the lungs of patients with *Cystic Fibrosis* and in chronic wounds. We could conclude that bacterial interspecies cell-cell communication through a membrane was possible in our setup. Further, a double membrane setup with a water phase in between the membranes, showed the same bacterial interaction. This last setup enabled molecular analysis of the water phase and thereby the signal molecules.

Acknowledgements

We want to send a big thank you to our committed and inspiring supervisors who believed in us and our project;

Sokol Ndoni, for his guidance and knowledge about block copolymers, Charlotte Frydenlund Michelsen, for teaching us all we know about bacteria and microbiology, and Claus Sternberg for support and ideas.

To Lars Schulte, for helping us with the polymer membrane production and characterization. To Lotte Nielsen, for teaching and helping us with MALDI-TOF analysis. To Tao Li, for helping us with additional SEM analysis. To all the members of the research group Self-organized nanoporous materials at DTU Nanotech. To Øresundståg and Skånetrafiken for bringing us to Denmark and back home safely.

A project about…

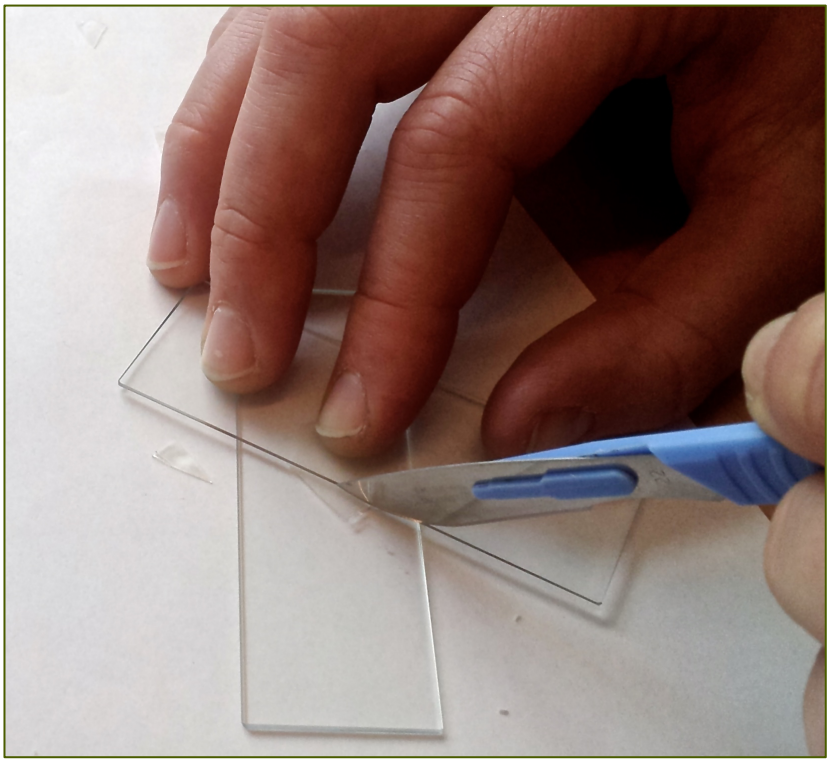

- Cutting-edge technology!

Table of Contents

1 Introduction

The research and development of microbiology have mainly been focused on single bacterial species. Still, many different bacterial species coexist in our ecological environment, for example is one gram of pristine soil occupied by over 1 million bacterial species (1). By secreting chemical compounds the bacteria perform cell-cell communication, not only with its own kind but also with other species (1), (2), (3), (4). Communicative interaction in between species makes polymicrobial communities a much more complex system to understand (1). There are two main kinds of interspecies interaction, 'cooperation' and 'competition', and both seem to be of great importance in the understanding of infectious diseases (2).

Studying bacterial interactions are most often done by co-colonization or cross streaking in petri dishes or by adding supernatant from one bacterial growth to another (4). Here, the usage of permeable membranes could be another way to retrieve information about the bacteria's signalling molecules. A membrane setup would allow physical separation of the bacterial species, meanwhile they are chemically connected by diffusion of signalling molecules through the membrane.

1.1 Membranes

Membrane technology is a fascinating field that enables advanced separation processes, and is often used in medical filtration, food processing and emission capturing (5). Classical filtration with porous membranes is pressure-driven, and the separation derives from the rejection of at least one component in a mixture when it flows through the membrane. Selection can be size-dependent or rely on electrostatic interactions (6).

To produce a membrane with desired attributes and thereby select what compounds the membrane can let through, the properties in Figure 1 should be well considered. The top row presents the properties that can be controlled in the fabrication. By controlling the fabrication the membrane properties in the bottom row can be achieved (5).

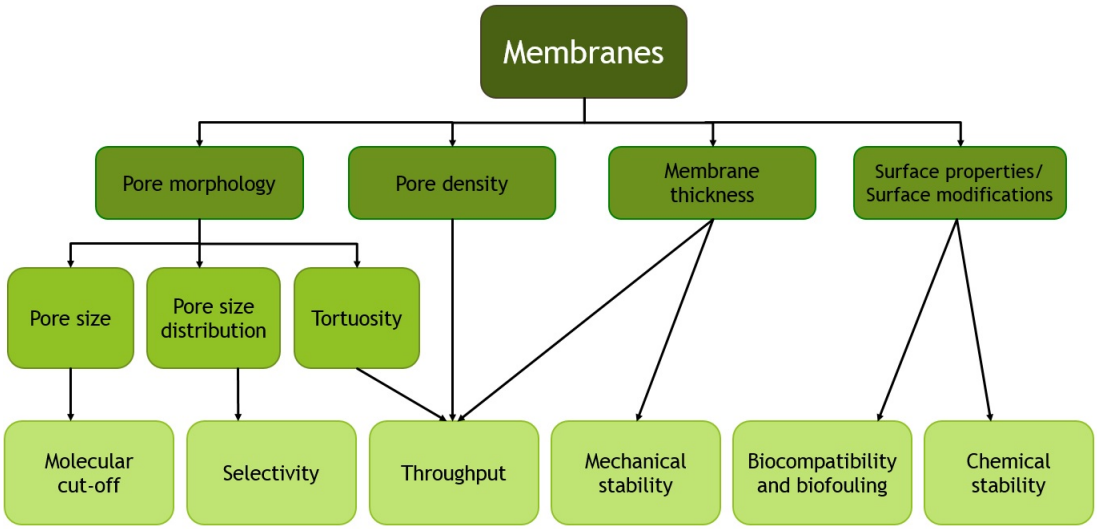

Figure 1: An overview of parameters that can be varied to obtain desirable membrane properties (5), (7).

In this project we have chosen two different kinds of membranes for the investigation of their performance when used in a membrane setup for bacterial growth. We used a block copolymer based membrane with a pore size of 10 nm and commercially available Millipore membranes with two average pore sizes of 220 and 450 nm respectively.

1.1.1 Block copolymer based membranes

Macromolecules referred to as block copolymers are composed of blocks of different polymers joined together by covalent bonds. Block copolymers with two blocks, diblock copolymers, can self-assemble in a range of different morphologies, Spherical (BCC), Lamellar (LAM), Hexagonal (HEX) and Gyroid (GYR). The morphology is influenced by degree of polymerization, composition, temperature and pressure. By removing one of the polymer blocks a nanoporous structure can be achieved. The nanoporous materials are of high interest as they have several applications e.g. in filtration, for medical diagnostics, as templates for electronics, in nano-reactors (8), in low dielectrics constant materials (8), (9) and in photonic materials (9). To enable the removal of one block the remaining polymer has to be mechanically stable. This is, in our case, realized by introducing a cross-linker that freezes the morphology, giving stability even at elevated temperatures and in contact with solvents (8).

1.1.2 Millipore membranes

Millipore membranes are commercially available filter membranes that can be ordered with different properties and in different setups. The ones with a pore size of 220 nm are, for example, often used for sterile filtration of liquids and are therefore available mounted in a device that can be connected to a syringe. The membranes are made of polyvinyl difluoride (PVDF), and provide a high flow rate combined with a lower attachment of proteins to the surface than nylon and nitrocellulose membranes. PVDF is a hydrophobic material, however, the Millipore membranes from Merck have a special surface modification rendering the pores hydrophilic (10).

1.2 Pathogenic bacteria in *Cystic Fibrosis*

Bacteria are often found in places where multiple bacterial species grow, and in these mixed-species environments they affect each other (4). Bacteria have the potential to read signals produced by other bacterial species in their proximity, also signals they do not produce themselves (1), (2). This kind of interspecies communication can contribute to enhanced virulence of the bacteria, bio-film formation and the development of antibiotic resistant polymicrobial communities (4), (11). Such an interaction has been seen between the two most common bacterial species infecting the lungs of *Cystic Fibrosis* patients, *Pseudomonas aeruginosa* (*P. aeruginosa*) and *Staphylococcus aureus* (*S. aureus*) (2), (4), (12).

Cystic Fibrosis (CF) is a genetic disease that leads to chronic inflammation in the lungs. It is caused by a defect in the gene encoding a cystic fibrosis transmembrane conductance regulator (CFTR), and is inherited by 1 in 2500 persons in EU. The CFTR is a membrane protein that transports chloride ions across the cell membrane in epithelial cells, and a malfunctioning protein results in a decreased quantity of periciliary fluid in the lungs. The periciliary fluid is required for the cilia to work properly. Cilia are needed to remove particles and microbial cells (mucociliary clearance) that are trapped in the mucus fluid. When this cilial clearance of microbial

cells is non-functioning, bacteria can start to colonize the lungs, causing an infection (13).

From the airway inflammation present in the early stage of CF, it is most commonly *S. aureus* that is found, the pink line in Figure 2. Young CF patients are therefore successfully treated with anti-staphylococcal antibiotics. However, when the patients acquire *P. aeruginosa* (the red line in Figure 2), *S. aureus* is cultured less frequently. Most important is that although *P. aeruginosa* has virulence factors that enable inhibition of *S. aureus*, both species are often still found together at the infection site. This correlates with the findings that *S. aureus* becomes resistant to several antibiotics when co-cultured with *P. aeruginosa* (12).

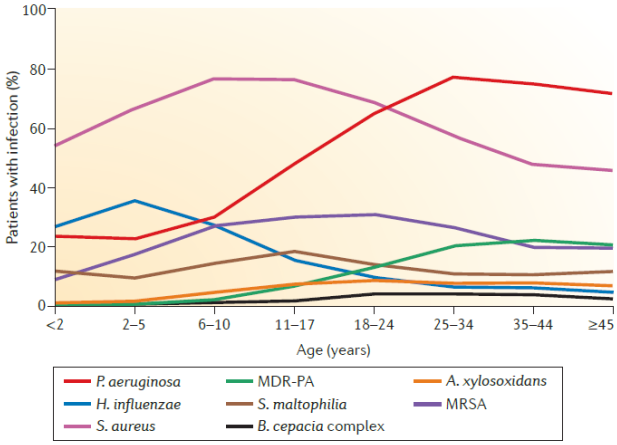

Figure 2: Prevalence of several common human respiratory pathogens in patients with cystic fibrosis (CF) as a function of age. Pseudomonas aeruginosa is the most frequently found pathogen in adults (13).

How the initial colonization of *P. aeruginosa* occurs is unique for every CF patient, but seems to come from unidentified environmental reservoirs. It has been seen that *P. aeruginosa* adapts to the stress in the lung environment to become more resistant (2), (4), (13), (14), (15). The initial intermittent colonization phase eventually transitions to a chronic infection, which is characterized by continuous growth of *P. aeruginosa* in the airways and by the development of *P. aeruginosa*-specific antibodies. This long-time infection affects the lungs and causes, both directly and via polymorphonuclear lymphocytes (PMNs), severe lung tissue damage (13). In these chronic infections *P. aeruginosa* cultures are characterized by slow growth, antibiotic resistance, lack of motility, loss of quorum sensing, changed cell envelope and overproduction of alginate (13).

Due to the severity of polymicrobial infections, such as the *P. aeruginosa* - *S. aureus* infection, in the lungs of CF patients, it is of great importance to find effective and reliable methods for the study of bacterial interactions. The objective of our study is therefore to develop and investigate a new technique for analysis of bacterial interactions.

1.3 Aim of project

The aim of this project is to combine a porous membrane with co-cultured bacteria. The membrane is used as a separating wall between the two bacterial species, which gives us the ability to discriminate what molecules that are able to go through at

chosen pore size and hydrophilicity of the membranes. It was suggested by Tashiro et al. (1) that micro-culture chambers with permeable walls allowing the study of multiple groups of organisms in a "spatially separated, yet chemically connected" manner is the ideal way to study cell-cell communication (1). Our membrane system differs from the micro-culture chamber proposed in (1), by being a macro-scale membrane chamber, however still permitting the study of diffusing signal molecules in a hydrophilic environment.

The purpose of studying the bacterial interaction between *P. aeruginosa* from CF patients (*P. aeruginosa* DK2) and *S. aureus* JE2 wild type (WT) is to find out what signalling molecules they exchange, as a way to find potential new strategies to reduce the severity of *P. aeruginosa* - *S. aureus* infections (16). Primarily, the focus of this work has been on the growth zone inducing agent from *S. aureus* to *P. aeruginosa* DK2 and the yellow pigment inducing agent from *P. aeruginosa* DK2 to *S. aureus*, see Figure 3, as reported by Michelsen et al. (4). These initial results, shown in Figure 3, have been used as reference for the identification of the growth zone in *P. aeruginosa* DK2 and the yellow pigment induction in *S. aureus*.

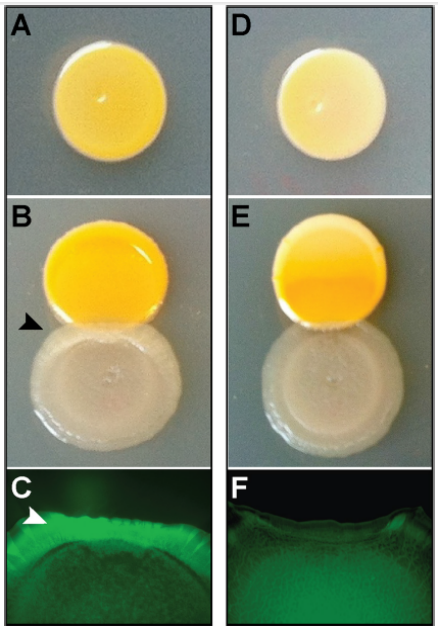

Figure 3: A) Monoculture of *S. aureus* JE2 (WT).
B) Co-culture with *P. aeruginosa* DK2-P24M2-2003/*gfp*AGA and *S. aureus* JE2, the black arrowhead indicates altered *P. aeruginosa* colony morphology.
C) The *Gfp* fluorescence signal of *P. aeruginosa* DK2-P24M2-2003/*gfp*AGA, after 3 days of incubation, is visualized in the zone of interaction with *S. aureus* JE2. The white arrowhead indicates increased *Gfp* expression.
D-F) The same experiment but with *S. aureus* mutant (*S. aureus* agrC), which is unable to induce enhanced growth in *P. aeruginosa* DK2. Therefore there is no fluorescence signal in F).

Moreover, the interactions between the *P. aeruginosa* WT, PaO1, and *S. aureus* JE2 WT were investigated for comparison. PaO1 is a *P. aeruginosa* strain that is found in the environment. It has a higher production of the green pigment pyocyanin and other virulence factors, more biofilm formation and higher motility than the *P. aeruginosa* DK2 strain that has evolved during chronic infections in CF patients (13).

1.3.1 Experimental design

In order to attain a good understanding of the project, we here explain the basic experimental design. The core of the experimental setup is a box with a membrane standing in the middle, see Figure 4. The box is built of object glass slides using a Formerol® clay called Sugru® to paste them together. A porous membrane, either a nanoporous or a Millipore membrane, is attached in the middle of the box and carefully sealed to the edges with Sugru. After sterilization the box is used as a bacterial growth chamber with the aim of studying the interactions between the two bacterial strains *P. aeruginosa* and *S. aureus*. The bacteria are cultured on either side of the membrane in order to separate them physically but let them be in chemical contact via diffusion across the permeable membrane.

In the beginning of the project, the intention was to have the nanoporous membrane as a central part of the experiments. However, the 10 nm pores are seemingly too small and effectively block the expected bacterial interactions, which is why the Millipore membranes account for a bigger part of the results in this project. In the report, we still write about the nanoporous membranes since they might have potential when other reactants are to be investigated.

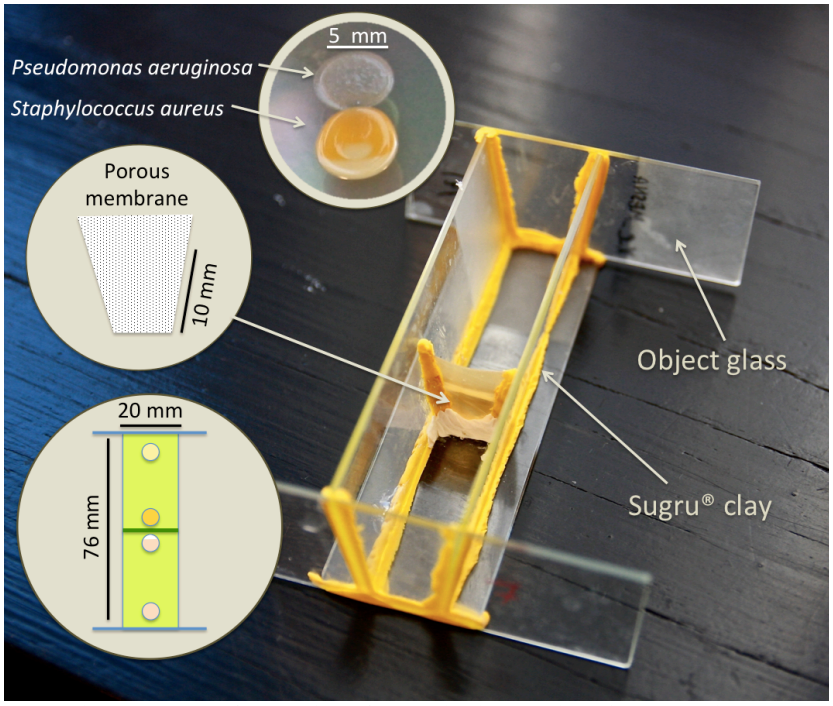

Figure 4: The experimental setup for studies of bacterial interactions in our project.

1.3.2 Workflow

To enable the reader to get an idea about the work presented in this report the workflow is displayed in Figure 5. The boxes in dark green represent the five main activities; membrane production, characterization and mounting, and bacterial growth and analysis. The boxes below, in light green, summarize the main steps and techniques applied in each activity. To ease the reading the report is organized according to the workflow, guiding the reader through the report.

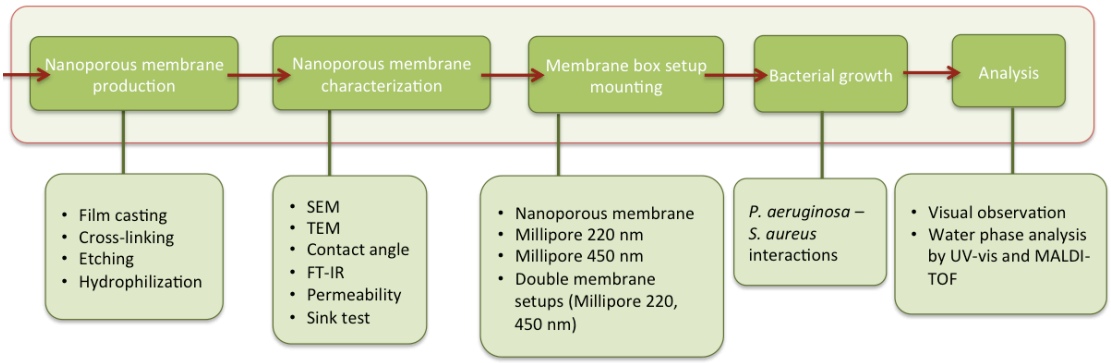

Figure 5: Scheme summarizing the workflow from the production of membranes to the analysis of bacterial growth, phenotypes and signal molecules.

2 Theory

2.1 Block copolymer based membranes

A macromolecule formed by two or more chemically homogenous polymer chains joined together by a covalent bond is referred to as a block copolymer. The diblock copolymers have been materials of great interest during the last 2-3 decades thanks to their phase behaviour leading to self-assembled morphologies. The microphase self-assembly is driven by an unfavourable mixing enthalpy and a small mixing entropy. Macroscopic phase separation is prevented by the covalent bond joining the blocks. The microphase separation gives a variety of morphologies, and it is dependent on the degree of polymerization, the block-affinity i.e the Flory-Huggins parameter, the volume fraction of the two constituent blocks, and the temperature and pressure. The microphase diagram below, Figure 6, presents the different thermodynamically stable morphologies for 1,2-polybutadiene-*block*-polydimethylsiloxane (1,2-PB-*b*-PDMS), as this is the block copolymer used in our study. The microphases are spherical (BCC), lamellar (LAM), cylinders (HEX) and gyroid (GYR) (17) and can be seen in the schematic microphase diagram in Figure 6. Hexagonally perforated layer (HPL) is a metastable phase (18) that is also present in the experimental diagram below.

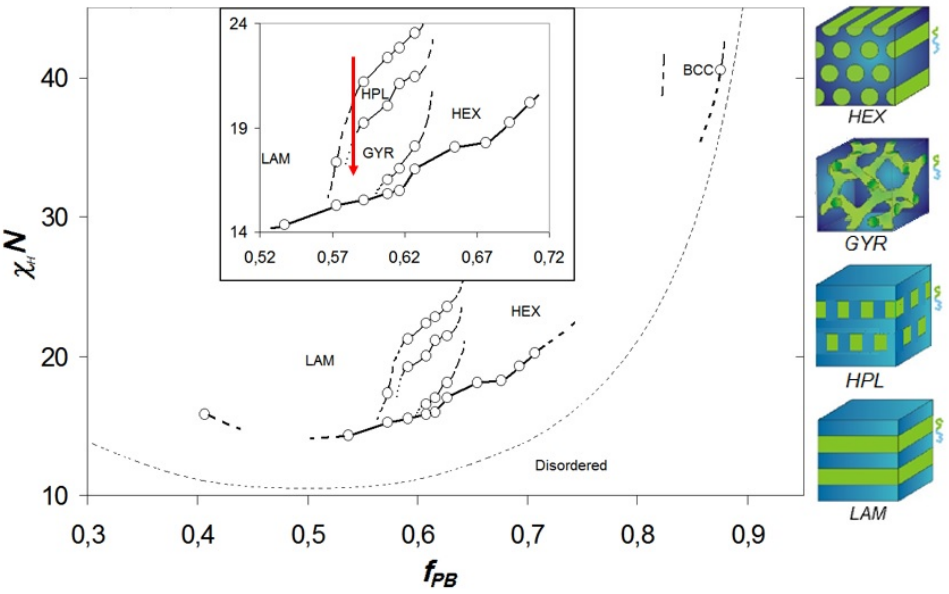

Figure 6: Experimental microphase diagram of linear 1,2-PB-*b*-PDMS block copolymers and representations of commonly observed morphologies. PB is blue and PDMS is green in the morphology schemes to the right. The red arrow represents the order-to-order transition (OOT) from lamellar (RT) to gyroid (140°C) for the block copolymer used in this project (19).

2.1.1 Polymerisation of block copolymers

There are many techniques to produce block copolymers, for example by coupling of homopolymers, by sequential anionic polymerization, by atom transfer radical polymerization (ATRP), by nitroxide-mediated polymerization (NMP) and by ring opening polymerization (ROP) (17). In this report we will describe sequential living anionic polymerization as it is the technique used to produce the polymers in this study.

Living polymerization is characterized by a reactive site that moves along the polymer chain during the polymerization. When all the monomers in the reactor are consumed the reaction will stop, but as soon as more monomers are added the polymerization continues, and therefore is said to be "living". This gives the possibility to store the polymer, for later use. Living polymerisation in the absence of chain transfer and chain termination provides well-defined polymer chains. There are two main conditions to achieve a well-defined polymer (i.e. with a very narrow molecular mass distribution) by anionic polymerization; an initiation step that is much faster than the propagation, and ideal mixing i.e. equal probability of chain growth at all reaction sites (20).

Sequential anionic polymerization can be used to produce block copolymers by simply exchanging the type of monomer introduced into the reactor. When the first block has reached a desired molecular weight, a different monomer is introduced giving a diblock copolymer. If the sequential addition is continued more complex multiblock structures can be formed (20). To make sure that the new kind of monomer will be coupled to the already existing chain, one have to follow the scale of reactivity; dienes/styrene > vinylpyridines > (meth)acrylates > oxiranes > siloxanes. The first block to be polymerized is the one that is composed of a monomer, which forms the most reactive propagating centre (17).

2.1.2 Synthesis of 1,2-PB-b-PDMS

In the case of 1,2-PB-*b*-PDMS, the most reactive monomer with respect to the scale of reactivity is butadiene, thus the first chain to be polymerized is the 1,2-PB. Butadiene can react on the sites of the double bonds i.e. 1,4 and 1,2 and the resulting polymers can be seen in Figure 7. The 1,4-PB (both cis and trans) reaction results in a polymer with a sterically hindered double bond, while the 1,2 configuration gives a primary double bond hanging down from the polymer chain. This double bond has barely any steric hindrance, making it more reactive than that of the 1,4 polybutadiene (21). The 1,2-polybutadiene, with its reactive double bond, is preferred for further functionalization. By using tetrahydrofurane (THF) as media for the polymerization the reaction of the 1,2-site is favoured (22).

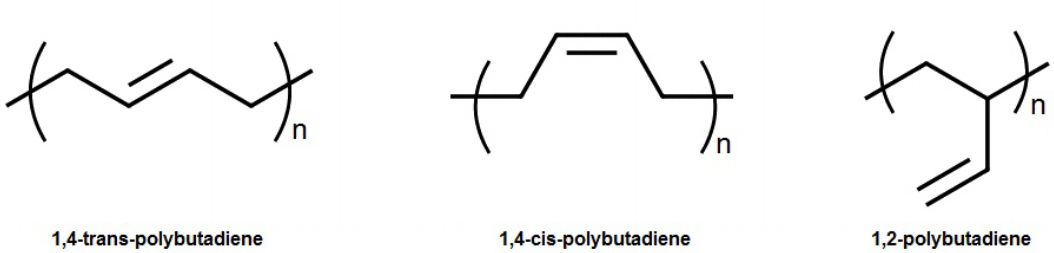

Figure 7: The different structures of polybutadiene.

To start the polymerization butadiene has to be initiated, which is done by adding the initiator sec-butyllithium (8), as shown in Figure 8. When sec-butyllithium reacts with butadiene it leaves a very reactive carbon that becomes the reaction site for further polymerization, see Figure 9 (23). The high reactivity of the reaction site is the reason why the polymerization temperature of 1,2-PB is kept below -20°C (8).

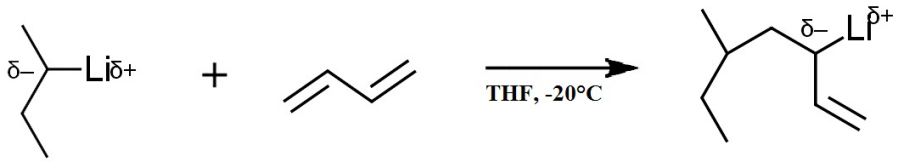

Figure 8: Initiation of butadiene.

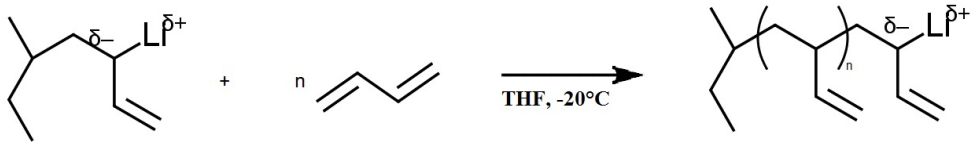

Figure 9: Propagation of butadiene to polybutadiene.

Once the desired chain length is reached i.e. all butadiene is consumed, the coupling and polymerization of the PDMS block can start, Figure 10. This is done by introducing a THF solution of the PDMS monomer hexamethylcyclotrisiloxane (D_3). The reactive site is then transferred to an oxygen atom in D_3, and this crossover is verified by the disappearance of the pale green-yellow color that is characteristic for the reactive carbon ion in PB. The temperature is then increased to 0°C and the polymerization continues (8).

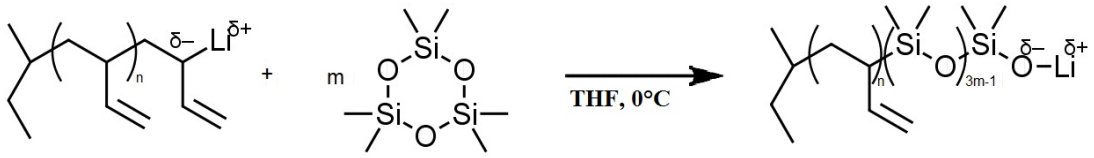

Figure 10: Propagation of D_3 to PDMS.

To terminate the polymerization, see Figure 11, trimethylchlorosilane (TMCS) is inserted to the reactor. The reactive oxygen will then attack and bind to Si in TMCS, leaving a methyl group at the end of the polymer chain. The polymerization is terminated and homogenous diblock polymers are retrieved (8).

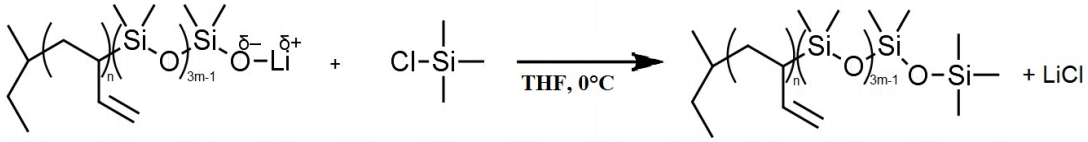

Figure 11: Termination of block copolymer.

*2.1.3 Fabrication of hydrophilic nanoporous membranes from 1,2-PB-b-*PDMS

A nanoporous membrane can be prepared by fabrication of a thin film from diblock copolymer, and removal of one of the blocks. As mentioned before the diblock copolymers self-assemble into different morphologies according to temperature and the blocks' volume fraction. All these morphologies; spherical, cylindrical and gyroid, can be used for making nanoporous structures. For our purpose the gyroid morphology is the most appropriate one as it gives open pores that percolate in all directions. With pores in all directions, there is no risk that the membrane surface is closed (24).

In Figure 12 the steps for fabricating hydrophilic nanoporous membranes are summarized. The initial step is the self-assembly of 1,2-PB-*b*-PDMS into the gyroid morphology, followed by the crosslinking of polybutadiene. After crosslinking the PDMS block is removed and finally the internal pore surface is hydrophilized (7). The process is further described in the following sections.

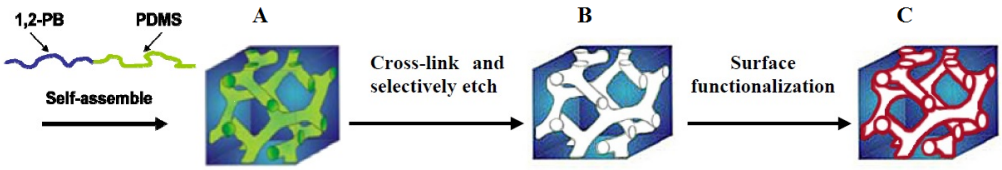

Figure 12: Schematic illustration of the fabrication of hydrophilic nanoporous 1,2-PB polymer membranes from 1,2- PB-*b*-PDMS block copolymer.
A) 1,2-PB-b-PDMS self-assembles into gyroid morphology.
B) PDMS is selectively etched away and a nanoporous polymer matrix is obtained.
C) The nanoporous polymer matrix is further modified via hydrophilization of the internal surface (7).

2.1.3.1 Cross-linking

To create a nanoporous structure, one first have to make sure that the matrix material is mechanically stable, otherwise it will collapse during removal of the etchable part. Mechanically stable blocks in block copolymers are typically crystalline polymers, glassy polymers or highly cross-linked polymers. In our setup it is important that the

polymer can withstand sterilization. Therefore a cross-linked matrix that enables the material to be stable in contact with solvent and at elevated temperatures is preferred. In the case of *1,2-PB-b-PDMS* it is the 1,2-PB block that is cross-linked, stabilizing the gyroid morphology at room temperature as explained below (8).

At room temperature the block copolymer is in the lamellar phase. When the temperature increases to 140°C the microphase transformes to gyroid as the $T_{ODT} \approx 100°C$ (8). Dicumyl peroxide (bis(a,a-dimethylbenzyl) peroxide, DCP) is a suitable cross-linker for PB, since it has an appropriate half-life at 140°C (25). When the temperature is increased to 140°C, DCP starts to crosslink 1,2 PB, preferentially at the vinyl sites and at the double bonds (8), according to the reaction schemes in Figures 13 and 14.

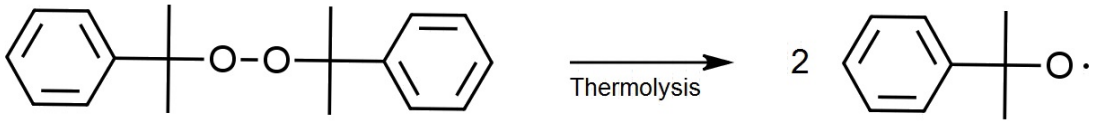

Figure 13: The activation of DCP, generating two alcoxy radicals that initiate the crosslinking of 1,2-polybutadiene.

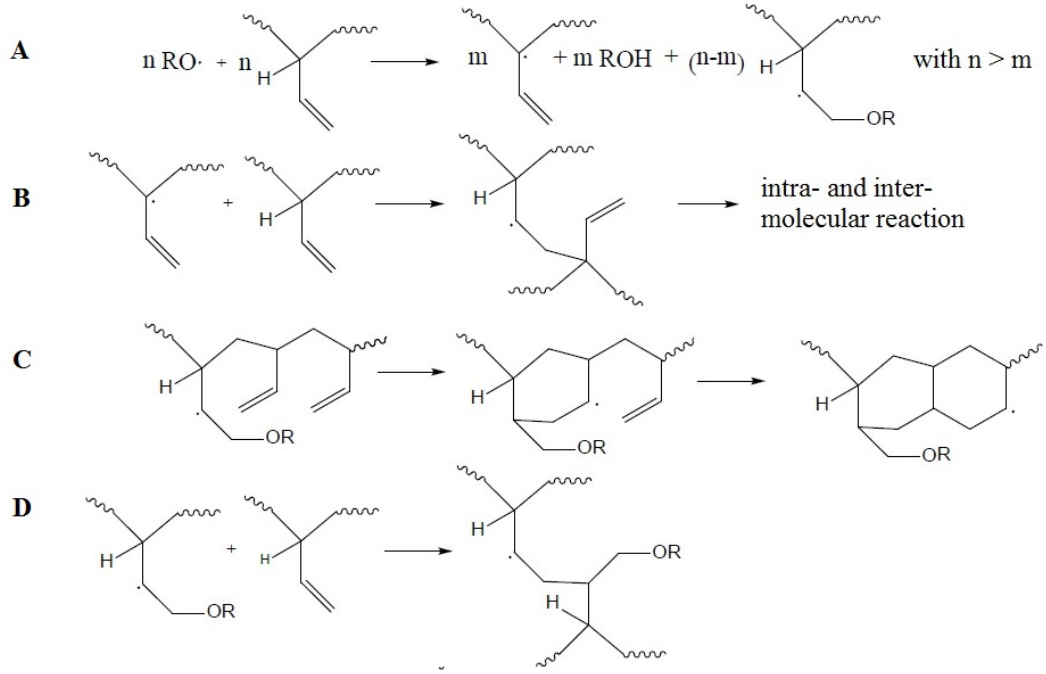

Figure 14: Cross-linking of 1,2-PB. A) Initiation of the reaction by the alcoxy radical, generating a free radical onto the polymer. Two products are achieved; radical on a tertiary (left) and secondary (right) carbon. Both can start a cross-linking chain reaction. B) The tertiary carbon free radical reacts. In C) and D) the secondary carbon free radical reacts (8).

2.1.3.2 Film casting

The surface morphology of a film cast copolymer is dependent on differences in interfacial energy between the selected substrate and the polymer. Therefore the material with which the polymer is in contact during cross-linking is very important. For example, glass has a much higher surface energy than either block and will therefore not appeal to any of them, resulting in a porous surface (non-skin surface). This will provide a gyroid structured surface that will have open pores after etching of the PDMS block (24).

If the polymer instead would be in contact with air, nitrogen or vacuum when cross-linked, the surface will get a non-gyroid skin layer at the surface. Air, nitrogen and vacuum have the lowest possible surface energy, and therefore the block with the lowest surface energy, PDMS, is more appealed to the surface than PB and create a skin-layer. This minimizes the air-polymer interfacial energy (7). Since the PB and PDMS blocks are coupled together by a covalent bond a layer of PB will form underneath the PDMS layer. The surface energy effect does not penetrate further down into the membrane film, hence the bulk morphology is gyroid (24). To get a gyroid structured surface without skin-layer, the surface can be sandpapered.

2.1.3.3 Etching of PDMS

A porous structure is achieved by removing one of the two blocks in a block copolymer material, see Figure 12. Selective etching of PDMS is performed using tetrabutylamonium fluoride (TBAF) in THF. TBAF degrades PDMS by cleaving the Si-O-Si bonds, (8), see Figure 15.

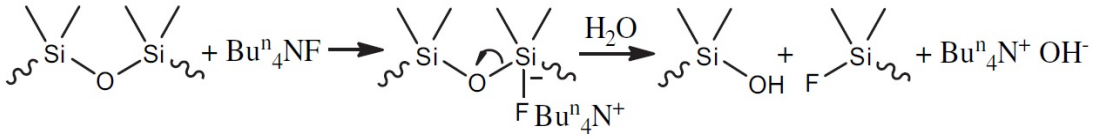

Figure 15: PDMS cleaving reaction mechanism by TBAF through the S_N2-Si pathway. The wavy lines depict the polymer chain (8), (26).

2.1.3.4 Hydrophilization

After etching of the PDMS block a large polymer-air interface is left inside the gyroid material. The surface area is estimated to around 280 m^2 per gram nanoporous gyroid polymer. The nanoporous interface consists of carbon, hydrogen and some fluoride, and they are all hydrophobic elements, rendering the membrane hydrophobic (27). The hydrophobic surface hinders water from filling the pores because of its high surface tension, giving a high contact angle and thereby a repelling capillary force, see Figure 16. In contrast, a pore with a hydrophilic surface, the capillary forces will drag an aqueous liquid into it (7).

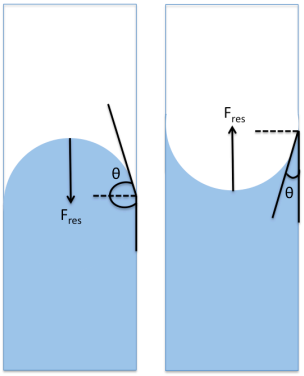

Figure 16: Capillary forces shown in a hydrophobic (left) and a hydrophilic (right) capillary. When the contact angle is larger than 90°, the surface is hydrophobic, resulting in a capillary depression. A hydrophilic surface will result in a capillary rise (7).

In our experiment, the objective is to make signalling molecules dissolved in aqueous media diffuse through a membrane, whereby the pore interfaces need to be

hydrophilized. This can be done by thiol-ene photo-grafting of sodium 2-mercaptoethanesulfonate (MESNA), which is a very efficient, specific and versatile method (27).

Thiol-ene chemistry is a kind of click reaction, which refers to reactions that have high yield, are regio- and stereo specific, works with several different starting compounds and are insensitive to oxygen or water. Further advantages with the chosen hydrophilization technique are that it is easy to use, efficient, homogenous and does not require special reaction conditions. Thiol-ene chemistry comprises a step-growth addition mechanism, where a thiol is initiated thermally or photochemically, creating a thiyl radical. The radical attacks a pendant double bond generating a vinyl radical. The vinyl radical reacts with a hydrogen from a free thiol, thus creating a new thyil radical, leaving a hydrophilic thiol at the polymer chain (27).

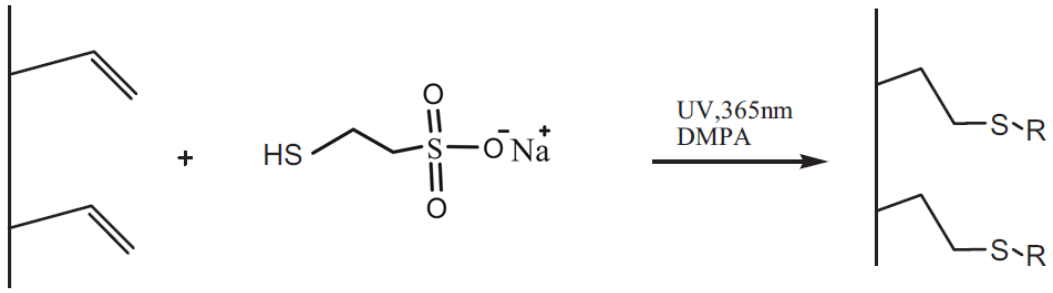

Figure 17: Reaction scheme for the thiol-ene click reaction (27).

After crosslinking and etching of 1,2-PB-*b*-PDMS, 30-50% of the double bonds in 1,2-PB are still free hanging and can be used for functionalization as hydrophilization. Here, MESNA is used to couple thiols to the polymer chain by thiol-ene chemistry, see Figure 17. To start the reaction the photo initiator 2,2-dimethoxy-2-phenylacetophenone (DMPA) is triggered with UV-light (27).

2.2 Millipore membranes

The Durapore® Millipore membranes, purchased from Merck, are made of PVDF, a fluorinated thermoplastic. The Millipore membrane microstructure can be seen in the SEM micrograph in Figure 18. Porous PVDF is a very stable plastic material that can withstand exposure to harsh thermal, chemical and ultraviolet conditions (28). The mechanical stability of PVDF is high even as thin membranes, which makes it easy to handle in different setups (29). The Millipore membranes are white and have a maximum operating temperature of 85°C, however they can stand one autoclave cycle up to 135°C. The Millipore membranes used in this study are hydrophilic due to surface modifications, 125 μm thick and have a (maximum) pore size of 220 or 450 nm (10).

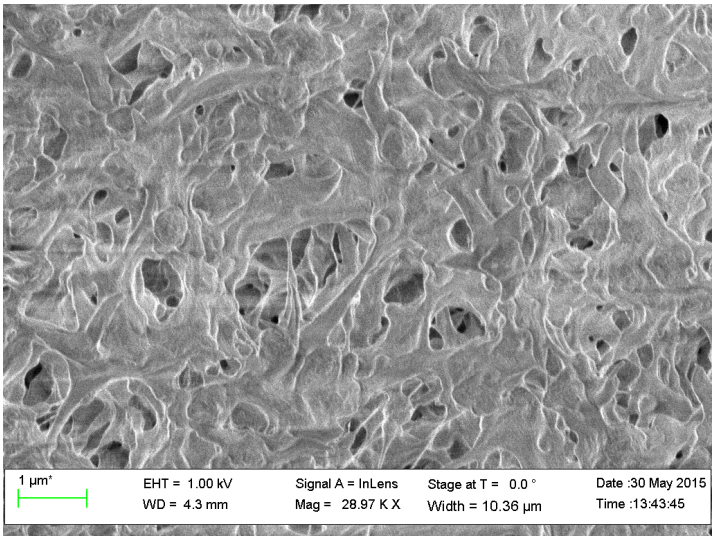

Figure 18: SEM image of the microstructure of the Millipore 220 nm membrane.

2.3 Human pathogenic bacteria

The interaction between human pathogenic bacteria is an important topic in the aim of understanding polymicrobial infection diseases, such as *Cystic Fibrosis*. Bacteria use small signal molecules to get information about their intracellular physiological status and extracellular environment (3). The extracellular signalling includes cell-cell communication, called quorum sensing (QS), which comprises the production, release and detection of signal molecules named auto-inducers. QS is used by the bacteria to monitor their population density and modulate gene expression accordingly (11). The auto-inducers from gram-negative bacteria are typically acyl homoserine lactones (AHL's) and alkyl-quinolones (AQ's), whereas gram-positive bacteria predominantly use modified peptides and amino acids (3), (11).

2.3.1 Staphylococcus aureus

Staphylococcus aureus is a common gram-positive bacterium that can be found on the human skin and in the respiratory tract of healthy people (30). Humans are natural reservoirs for *S. aureus* and it has been estimated that 20-30% of the healthy population are carriers (31). *S. aureus* is a spherical bacterium with a diameter of 1 μm (31) and it is a member of the Micrococcacea family (32).

To withstand stressful environments as anti-oxidative mechanisms and membrane-disrupting antimicrobial peptides, *S. aureus* produces the virulence factor staphyloxanthin, a pigment that turns the bacterial colony yellow (33). The color is unique for its kind and used as a means to distinguish *S. aureus* from other staphylococcal species (31), (32). In this study it is the induction of the yellow pigment staphyloxanthin in *S. aureus* that is investigated.

S. aureus is an opportunistic pathogen of humans and can travel with the blood stream and thereby infect almost every part of the body (30). The infections vary in severity and are a common reason for hospitalization (31). Because of *S. aureus* potential to develop antimicrobial resistance, it has established a resistance to several therapeutic agents throughout the years. Due to this fact it is important to study the mechanisms of *S. aureus* infections to enable the development of potential new effective therapies (31).

2.3.2 *Pseudomonas aeruginosa*

P. aeruginosa is a gram-negative bacterium that is found in our environment. It is rod-shaped and measures 0.5-0.8 μm in diameter, 1.3-1.5 μm in length and its single polar flagellum makes it a really fast swimmer (34).

P. aeruginosa is most commonly recognized for causing opportunistic infections and being the bacteria that resides in chronic wounds and in the lungs of CF patients (1) (14), (35). *P. aeruginosa* can grow in conditions with very low oxygen levels and at a temperature up to 42°C and is therefore found even in man-made environments (34). It accounts for a large number of nosocomial and hospital-acquired infections (16), and is good at imposing on a weakened immune system (34). *P. aeruginosa* is exposed to stress by interactions with the environment and other bacteria. This stress selects for mutants of *P. aeruginosa*, which adapt the bacterial strain to its environment (1). Antibiotics are used to treat *P. aeruginosa* infections in CF patients, and at present these patients can live to the age of 40 thanks to this. However, antibiotics impose stress on *P. aeruginosa*, and does therefore play an important role in the evolution of *P. aeruginosa* (13), (14).

2.3.2.1 *Quorum sensing system in P. aeruginosa*

The QS system in *P. aeruginosa* is controlled by two systems, the *rhl* and *las* system and the 4-hydroxy-2-alkylquinolone system (HAQ) system. The *rhl* and *las* system is induced by cell-density-dependent acyl-homoserine lactones (AHL) (4), while the HAQ system uses over 50 different quinolones for signalling, including 2-hydroxy-4-quinolone (HHQ) and 2-heptyl-3-hydroxy-4-quinolone (*Pseudomonas* quinolone signal, PQS) (36).

PQS is a molecule with a large impact on the QS system. PQS controls the expression of genes required for production of virulence factors and biofilm formation by inducing the transcriptional regulator *pqsR*. The biological precursor of PQS, HHQ, does also function as a signalling molecule. It has been found that HHQ can affect other bacterial species (35), by for example repressing bacterial motility and may also induce the production of the yellow pigment staphyloxantin in *S. aureus* (2).

The biological synthesis of HHQ is a condensation reaction of anthranilic acid and a β–keto acid, catalysed by the enzyme encoded by *pqsA*. *PqsA* is the first gene in the *pqsABCDE* operon, where the enzymes encoded by *pqsA-D* are required for the HHQ synthesis and the *pqsE* encoded enzyme is responsible for activation of PQS, see Figure 19 (37). *P. aeruginosa* with a mutation in *pqsA* is unable to produce both HHQ and PQS, which also leads to a lack of production of several virulence factors and toxins. The *pqsH* gene is somewhat extended from the *pqsA-E* operon, but has a key role: it catalyses the conversion of HHQ to PQS in the presence of molecular oxygen. A *pqsH* deficient mutant can thus produce HHQ but not PQS (37).

The *pqsH* gene encoding the enzyme that converts HHQ to PQS is under control of the *lasR* gene, connecting the AHL and the HAQ regulatory systems of QS (4). A *lasR* mutant *P. aeruginosa*, as *P. aeruginosa* DK2, will thus have an accumulation of HHQ. However, it has been shown that even in a *lasR* mutant PQS can be produced,

indicating either that *pqsH* can be *lasR* independent, or else that there is another enzyme (not encoded by *pqsH*) that can accomplish the PQS synthesis (38).

2.3.2.2 The kyunine pathway in prokaryotes

The kyunine pathway is an enzymatically catalysed reaction responsible for breaking down tryptophan into other compounds in eukaryotic cells. The same pathway in prokaryotes is less well known. It has been found that *P. aeruginosa* has genes encoding for proteins that are homologous to the enzymes in the eukaryotic kyunine pathway. These genes, *kynA*, *kynB* and *kynU*, encode a step-wise conversion of tryptophan to anthranilic acid, see Figure 19. Anthranilic acid can then be converted to HHQ by addition of a fatty acid (35). To conclude this, Farrow et al. (35) grew *P. aeruginosa* cultures in the presence of radio labelled tryptophan and after 24 h the cultures were extracted and analyzed with thin layer chromatography (TLC). The PQS location was marked and upon exposure to X-ray film it was concluded that the PQS molecules were radio labelled, proving that the tryptophan had been converted to PQS. Farrow et al. also showed that in *P. aeruginosa* mutant strains lacking *kynA* or the *kynU*, there was no PQS production, and in the *kynB* mutant only very little PQS was produced (35).

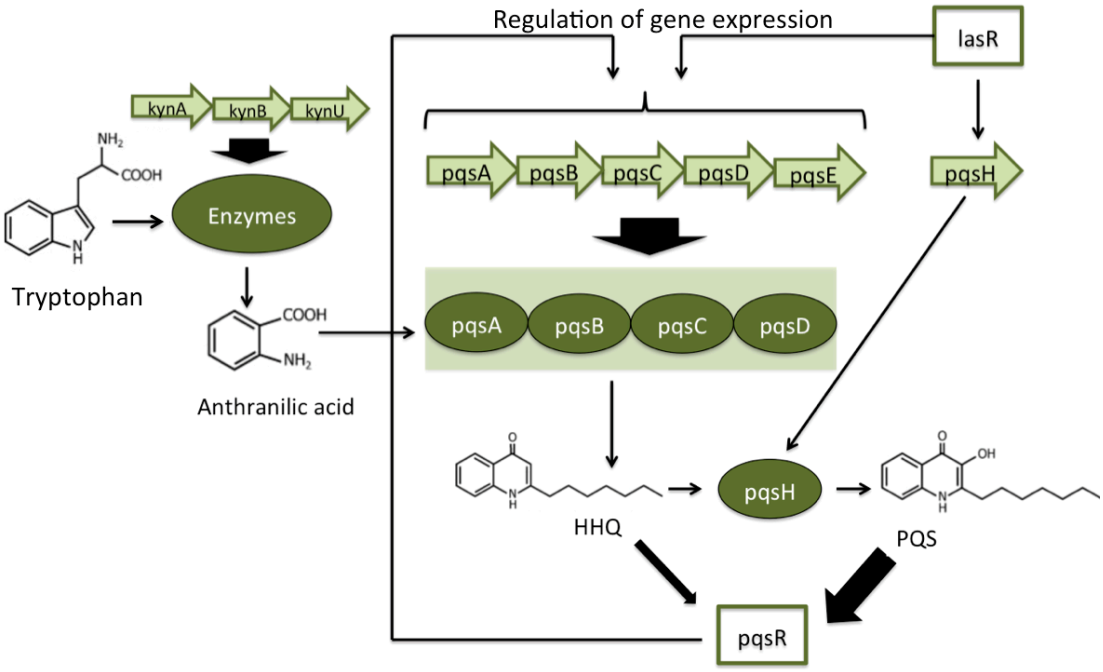

Figure 19: Scheme of the HHQ and PQS pathway and regulation. Trypophan is a precursor to PQS via the kyunine pathways that is expressed by the genes *kynA*, *kynB* and *kynU*. The genes in the *pqsABCDE* operon encodes the enzymes that converts anthranilic acid to HHQ, and *pqsH* for its further conversion to PQS. The expression of *pqsABCDE* is regulated by *pqsR*, which is activated by PQS itself, and to some extent also by HHQ. *LasR* regulates the expression of *pqsABCDE* as well as the expression of *pqsH*. *LasR*-mutated strains, as *P. aeruginosa* DK2, have less expression of *pqsH* and cannot convert HHQ to PQS and therefore shows an accumulation of HHQ. Labelled arrows represent genes, circles represent enzymes and boxes represent regulatory genes.

2.3.2.3 Vesicle transportation

The PQS molecule has a hydrophobic nature due to its long carbon chain. It has low solubility in water but is easier solubilized when rhamnolipids (biosurfactants) are

secreted. The regulation of rhamnolipid production in *P. aeruginosa* is, conveniently enough, dependent on the *rhl* QS, which is under control of PQS, meaning that PQS can control its own solubility (38). Another observation concerning the solubility of PQS was made by Mashburn et al. 2009 (39), suggesting that over 95% of the naturally produced PQS is associated with membrane vesicles (MV). In the same study, they show that the third-positioned hydroxyl group is required for MV formation, while the length of the second-positioned alkyl-group impacts the PQS potency to form vesicles (39). The HHQ molecule, which differs from the PQS molecule in its lack of the third-positioned hydroxyl-group, showed a significantly lower potency of inducing MV formation (39).

2.3.3 Staphylococcus aureus and Pseudomonas aeruginosa interactions

Many gram-negative bacteria, e.g. *P. aeruginosa*, show induced production of extracellular virulence factors when co-cultured with gram-positive bacteria (4), (12), (33). Thus in such polymicrobial infections synergy can be achieved, resulting in more resistant bacterial colonies, which single bacterial colonies are not able to attain alone. The interaction between *P. aeruginosa* and the gram-positive bacteria *S. aureus* has been shown to enhance wound severity, making the bacteria more resistant to antimicrobial treatment and causing a very slow wound healing. The virulence of *P. aeruginosa* is clearly increased at infection sites where *S. aureus* is present, which motivates the study of their interaction and the signalling molecules that are involved, in order to find better treatments for the diseases they cause (16).

P. aeruginosa isolated have been collected from Danish CF patients for over three decades, which has enabled studies (4), (36), (40) of the evolution of the bacterial lineages, one of them being the *P. aeruginosa* DK2 (4), (36), (40). The interaction of *P. aeruginosa* DK2 and *S. aureus* WT is strain dependent. When the early adapted *P. aeruginosa* DK2 strain is co-cultured with *S. aureus* WT, *P. aeruginosa* inhibits the growth of *S. aureus*, to the same extent as the *P. aeruginosa* PaO1 reference strain, meaning that there is a clear antagonistic interaction. However, when the same test is performed with the late adapted *P. aeruginosa* DK2 strain, there is a more commensal-like interaction and no inhibition of *S. aureus*. Extracellular factors from *S. aureus* have been found to enhance the growth activity in the late adapted *P. aeruginosa* DK2. This can be seen by visual observation of the bacterial morphology or by using fluorescence microscopy, see Figure 3. At the same time, *P. aeruginosa* exposes *S. aureus* to stress and thereby stimulates production of the yellow pigment staphyloxanthin. The color change in *S. aureus* from white to yellow is clearly visible after the incubation (4).

In the article by Michelsen et al. (4) the evolution of the *P. aeruginosa* DK2 lineage is studied. A mutation in the regulator *lasR* is frequently detected and this mutation is recognized by a distinct colony morphology showing “iridescent metallic sheen coverage” and zones of autolysis, both due to an accumulation of HHQ. The *lasR* mutation also causes decreased production of virulence factors. This is a very important evolutionary step for *P. aeruginosa* in its host adaption and could as well be beneficial for interactions with other bacterial species. When *P. aeruginosa* and *S. aureus* are co-cultured, *P. aeruginosa* develops a zone with a morphological change closest to the *S. aureus* colony. The zone arises due to increased growth rate or increased cell density, which has been concluded by the introduction of a

chromosomal *Gfp*-tag on a growth-dependent ribosomal promoter being able to discriminated between fast- and slow-growing cells. When observed visually the growth zone looks densely white, and it corresponds to the same area that fluoresces in green when observed with a fluorescence microscope, as seen in Figure 3 in the introduction. The interaction also showed a suppression of metallic sheen and a flatter surface with less autolysis when supernatant from an *S. aureus* culture was added to a lawn of *P. aeruginosa* (4).

Previous attempts (14), (15) have been made to identify the compound from *S. aureus* that induce the *P. aeruginosa* growth zone but without success. Palmer et al. (14) presented a study where the nutritional conditions in airway sputum were suggested to be a key parameter for increasing *P. aeruginosa* growth. They showed that amino acids were an important carbon source for *P. aeruginosa*, since metabolized carbon is a limiting factor for *P. aeruginosa* growth (14). In another study by D'Argenio et al. (15), it was shown that *lasR* deficient *P. aeruginosa* strains (as *P. aeruginosa* DK2) have an enhanced ability to use amino acids as nutrients. Their results showed that *P. aeruginosa* grown with the aromatic amino acid phenylalanine, displayed a growth advantage and reached a higher colony density. The growth advantage was reported to be specific for particular carbon sources, as the succinate grown *P. aeruginosa* did not express enhanced growth (15). It was also reported that the growth advantage of *P. aeruginosa* CF isolates was more pronounced in the late adapted *lasR* mutant than the early adapted (15). Thus release of amino acids from *S. aureus* could be a potential parameter for the increased *P. aeruginosa* growth phenotype observed during interaction in our setup.

Another interaction between *S. aureus* and *P. aeruginosa* has been shown to be communicated via peptidoglycans from *S. aureus*. The peptidoglycan component N-acetylglycosamine (GlcNAc) is a part of the cell wall polymer in gram-positive bacteria (16). Korgaonkar et al. report in their study (16) that GlcNAc enhances pyocyanine production in *P. aeruginosa*. *P. aeruginosa* senses and responds to the peptidoglycans from gram-positive bacteria by enhanced production of virulence factors, thereby enhancing *P. aeruginosa* pathogenesis. The production of pyocyanine in *P. aeruginosa* is controlled by the QS system and the PQS molecule, which was proved by a significant increased PQS production when *P. aeruginosa* was grown with GlcNAc (16). Gram-positive bacteria are found in most host tissues and they shed 25% of their cell wall during growth, providing *P. aeruginosa* with GlcNAc that makes *P. aeruginosa* more lytic for the gram-positive bacteria. Killed gram-positive bacteria will then provide even more peptidoglycan to *P. aeruginosa,* and this feedback loop was reported to result in a significant decrease of gram-positive bacteria during co-infections with *P. aeruginosa* (16).

2.4 Characterization methods

2.4.1 Electron microscopy

With electron microscopy objects on a smaller scale than with light microscopy can be observed. This is due to the shorter wavelength of electrons compared to light, which enables a higher resolution. Electrons are extracted by high voltage and accelerated by the electron gun, generating the electron beam that is focused onto the sample by several magnetic lenses. The imaging is carried out under vacuum and the interaction of the electron beam with the sample produces several types of signals, that are detected by various detectors. The signals are processed by a computer software in order to obtain the sample image (41), (42).

Scanning electron microscopy (SEM) is a surface analysis technique in which the focused electron beam is scanned across the sample. Electrons that are used for imaging are mainly secondary and backscattered electrons (41). In transmission electron microscopy (TEM) the sample needs to be very thin, to enable the electrons to be transmitted. The electrons that pass through the sample are detected and used for imaging (42).

2.4.2 FT-IR

Fourier Transform Infrared Spectroscopy (FT-IR) is a characterization technique based on the absorption in materials of electromagnetic radiation at different wavelengths in the IR range. The analyzed material will absorb light at frequencies that correspond to the vibrational mode frequencies of the molecular structure. This is measured using an interferometer and a computer software that converts the raw data to a spectrum via the Fourier transform (43).

In conventional FT-IR the signal depends on the thickness of the sample, since more material will absorb more energy. Attenuated Total Reflectance (ATR), see Figure 20, is an FT-IR technique that only goes 0.5-5 μm into the material. The infrared beam has a high incident angle and passes a crystal with a refractive index that is higher than that of the analyzed material, so that total reflection occurs. When the internal reflection at the crystal surface takes place, an evanescent wave is extended past the interface, protruding the material that is in close contact. Attenuation of the evanescent wave energy due to absorption in the material is then detected in the collected infrared beam (44).

The ATR FT-IR is convenient when solid materials are to be examined. Characteristic spectra from different materials are easily interpreted and added or removed chemical compounds can be visualized by comparing the spectra before and after chemical treatment.

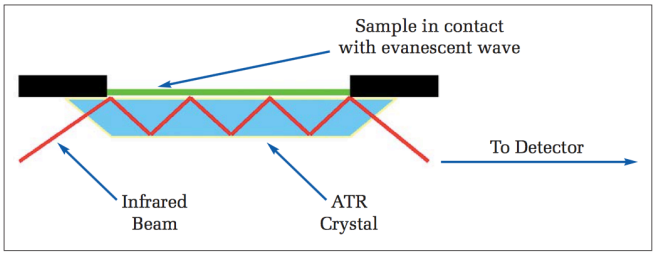

Figure 20: Schematic picture of the ATR technique (44).

2.4.3 Contact Angle

Measuring the contact angle (CA) of a water droplet on a surface is an easy interpreted method to determine if the material is hydrophilic or hydrophobic. The angle between the material surface and the edge of a deposited droplet is measured. Materials with a CA above 90° can roughly be considered hydrophobic, whereas materials with a CA below 90° are of more hydrophilic nature (45).

2.4.4 UV-Visible spectroscopy

UV-Visible spectroscopy (UV-Vis) is a technique that can be used to analyze liquid samples. This is done by focusing monochromatic UV-Vis light into a cuvette containing the sample and measuring the amount of transmitted light. By adding a second cuvette containing pure buffer and using a split beam, the background absorbance from the buffer can be subtracted. UV-Vis is an advantageous method for biomolecule identification as it requires small amounts of sample and is easy to use (46).

2.4.5 MALDI-TOF MS

Matrix-Assisted Laser Desorption Ionizer (MALDI) is a mass spectrometer technique that enables intact proteins and other large biomolecules to be detected and recognized from their mass over charge ratio (*m*/*z*). The sample is mixed with a matrix and they are co-crystallized on a sample plate. The matrix should be a small acid molecule with its principal attribute that it has high absorption of UV-light from the laser. The matrix molecules absorb the laser energy and convert it to heat, which desorbs the surface molecules of the matrix-sample-mix. The vaporized molecules, charged from the acid matrix molecules, are accelerated over a potential and the time of flight (TOF) that it takes each molecule to reach the detector is measured. Molecules will then have a TOF corresponding to their respective mass-charge ratio (*m*/*z*), generating a mass spectrum of the sample. MALDI is a sensitive tool for rapid analysis that gives accurate results. It is convenient that no sample preparation steps are needed but the matrix mixing, and that a wide range of molecular masses can be detected (1-300 kDa). The molecules that were searched for in this study have an *m*/*z* lower than 1 kDa, which is in the same range as the matrix molecules. Nevertheless, the MALDI-TOF MS settings can be optimized for acquiring lower *m*/*z*, but the automatic matrix suppression cannot be used (47).

2.5 Materials

2.5.1 Sugru

Sugru was used to seal the membrane box setup and to attach the membranes. The Sugru clay, Figure 21, is principally made of talc (25-50%), barium sulphate (15-25%) and silicon dioxide (5-10%). It is a rubbery clay that is easy to form and attaches good to many materials, and it hardens in 24 hours (48).

Figure 21: The Sugru clay (49).

3 Method

3.1 Experimental setup

The growth chamber device had to fulfil three criteria; it had to stand sterilization, it should be easy to attach the membranes and exchange them after use, and it had to allow good visibility e.g. for top-down imaging of the bacterial growth.

This drove us towards a growth chamber design that we could easily produce ourselves, made of object glasses sealed together with the silicon clay Formerol® (trade name Sugru®), see Figure 4. The membrane was sealed to the glass box with Sugru in the same way. Since the membrane is a very brittle material, this attachment was a difficult step, and was therefore facilitated by tilting the sidewalls of the growth chamber box.

3.1.1 Membrane box setup

Different membrane systems were used as an attempt to capture different signalling molecules according to their sizes. Two setups with nanoporous membranes (with a pore size of 10 nm) were used, a single membrane setup and a double membrane setup, Figure 22. The column between the membranes in the double membrane setup contained distilled, sterilized water. For larger pore size, Millipore membranes with a pore size of 220 and 450 nm were used, both in single and double membrane setups respectively. For comparison of the bacterial phenotypes, a control colony was spotted with greater distance to the membrane. A control box without membrane between the co-cultured bacterial spots was always used. Spot-cultured petri dishes were also used as controls.

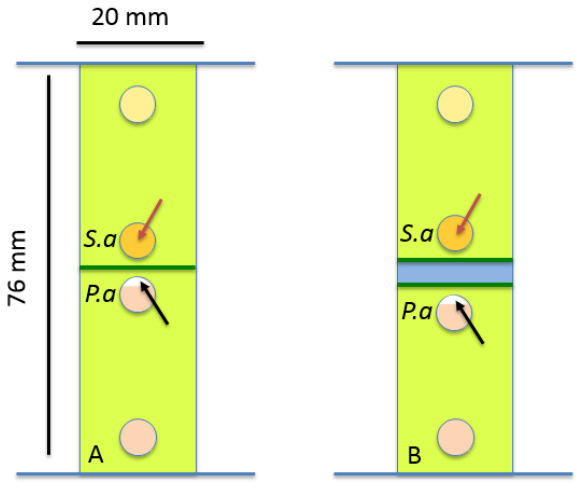

Figure 22: Membrane box setups and the possible colony morphologies of *S. aureus* and *P. aeruginosa* after incubation, see Figure 3. The red arrows indicate the yellow pigment induced phenotype in the *S. aureus* colony and the black arrows indicate the growth zone induced in the *P. aeruginosa* colony. A) The single membrane setup and B) the double membrane setup with a water phase between the two membranes.

3.2 Production of nanoporous 1,2-PB membranes

3.2.1 Polymerization

The block copolymer is synthesized under argon atmosphere by living anionic polymerization. Sec-butyllithium was used as an initiator and THF as medium for the polymerization of the two blocks. The polybutadiene block was synthesized at - 20°C for 3 h, and then the PDMS monomer hexamethylcyclotrisiloxane (D_3) was inserted to the reactor. The temperature was increased to 0°C and the polymerization continued for three days. To terminate the block copolymer chains, a three times excess of trimetylchlorosilisane was added (8). Finally the polymer with a molecular weight of 15 kg/mol was rinsed in methanol and dried under vacuum overnight.

3.2.2 Film casting

To calculate the material needed for a desired final membrane thickness the diameter of the petri dish used as template was measured. From this information the total volume of polymer was determined.

Two types of 1,2-PB-*b*-PDMS (BD) were used, 40% BD44 ($\bar{M}_n$ = 30 700 g/mol, PDI = 1.03) and 60% BD49 ($\bar{M}_n$ = 16 400 g/mol, PDI =1.05). The densities of PB (ρ = 0.90 g/cm^3) and PDMS (ρ = 0.97 g/cm^3) are quite similar and the mass fraction between the two blocks is therefore almost similar too (50), which is why the approximation 1 cm^3 ~ 1 g polymer was made. The volume of polymer can then easily be converted to the required amount of polymer.

The polymer was put into a glass vial. To enable the crosslinking, 1.5% mole DCP was added in proportion to the molar amount of double bonds in the 1,2-PB block. The polymer was dissolved in THF to realize a concentration with 20% polymer. The solution was film cast in a petri dish and left overnight to let the THF evaporate.

To avoid skin-layer formation on the polymer film a petri dish with a slightly smaller diameter than the template petri dish was pressed down into the film. To prevent pushing the petri dish too deep into the polymer, spacers were placed in cut holes in the polymer film. The petri dish was then inserted into a steel cylinder and flushed with nitrogen to avoid oxidation. Next, the cylinder was put into an oven at 140°C for 70 minutes. The steel cylinder was not opened before it had cooled down, to avoid that the membrane oxidize. After cooling, the petri dish was left in the refrigerator to ease the detachment of the polymer film.

3.2.3 Etching of PDMS

To open up the gyroid structure and achieve 10 nm pores the PDMS, which counts for 40% of the total weight, was etched away using a solution of 0.5 M TBAF in THF. The cross-linked membrane was put into a glass jar and the TBAF solution was added at 3 times molar excess relative to the concentration of the repeating unit in PDMS. The membrane was left to etch on a shaking plate for 36 h. After etching the membrane was rinsed for 30 minutes in five different solutions of THF and ethanol. The concentrations of the solutions were: 100, 75, 50, 25% THF in ethanol and finally 100% ethanol. The membrane was left to dry between two filter papers clamped together by two glass slides.

3.2.4 Hydrophilization

The membranes were hydrophilized by thiol-ene click chemistry, using the free hanging double bonds in the polybutadiene block to attach hydrophilic thiols. First a solution of 70% ethanol in water with a volume enough to cover the membrane was thoroughly mixed with 1 mM photo initiator, DMPA (2,2-dimethoxy-2-phenylacetophenone, M_W = 256.3 g/mol), and 0.5 M hydrofilizer, MESNA (M_W = 164.18 g/mol). The solution was poured into a plastic box containing the membranes and left for 2 hours to ensure a uniform distribution of the solution in the pores. To minimize the light inlet and avoid premature initiation of the reaction the box was covered with aluminium foil and placed in a carton box. The hydrophilization was conducted using a UV-light setup. The lid of the foliated box was replaced by a glass-slide to prevent evaporation and the UV light (315-400 nm) was turned on for 30 minutes. After hydrofilization the membrane was rinsed in 70% ethanol for 15 minutes, three times.

3.3 Characterization of membranes

3.3.1 Scanning electron microscopy

In order to visually observe the membrane surface and its structure, samples were mounted with carbon tape on sample holders and grounded using copper tape for better conduction and decreased sample charging. Before analysis all samples were sputtered with gold in a Cressington 208 HR sputter coater at 300 mA for 5 seconds. Insulating samples will accumulate the electrons from the beam, as they are unable to conduct electrons, and result in charging effects. Therefore, all organic samples are coated with a thin layer of gold before SEM analysis. The SEM imaging was done with HELIOS or Quanta 200F instruments from FEI, with an acceleration voltage of 3, 5 or 10 kV.

3.3.2 Transmission electron microscopy

For further imaging, especially of the cross-section of the polymer film, TEM was used. The samples were prepared at room temperature using a Leica ultracut UCT ultramicrotome with a cryo 35 diamond knife (DIATOME). The samples were 90 nm thick and applied onto a copper grid that was mounted onto the sample holder. The TEM imaging was performed with an acceleration voltage of 200 kV in a FEI TECNAI G2.

3.3.3 FT-IR

FT-IR was used to determine the composition of the polymer membrane in the different steps of the synthesis i.e. crosslinking, etching and hydrophilization. The measurements were conducted using a Perkin Elmer Spectrum 100 FT-IR Spectrometer with a Universal ATR sampling accessory.

3.3.4 Contact Angle

The contact angle (CA) of water on the polymer membranes was measured using a Contact Angle System OCA 20. A droplet with a volume of 3 μl was deposited onto the surface and a camera showed a close-up picture of the droplet profile. The measurements were performed at room temperature using the sessile drop method.

3.3.5 Sink test

To conclude whether the membranes were hydrophilized and porous or not a standardized sink test was introduced. Etched hydrophobic samples were put into a vial with methanol to a height of 5 cm. The time it took for the membrane to sink was measured. For etched, hydrophilic samples the test was performed in water. This is possible because the density of 1,2-PB increases to slightly more than 1 g/cm^3 during crosslinking, rendering a porous polymer filled with water denser than pure water.

3.3.6 Permeability test

To conclude whether the pores of the produced membranes were open and if the membranes were permeable in an aqueous solution, a standardised method was used. After mounting the membrane in the box setup, a 0.1 M solution of KOH was poured on one side of the membrane and on the other side a 1 mM solution of phenolphthalein in isopropanol and water (1:10). Phenolphthalein is a pH indicator that changes from transparent to strong pink at pH above 8.2. If the membrane is permeable and hydrophilic, the colorless phenolphthalein will come in contact with the strong basic solution and turn pink.

3.4 Investigation of *P. aeruginosa – S. aureus* interactions

The membrane boxes were prepared with membranes the day before culturing, to ensure that the Sugru clay had hardened. 200 ml LB (Luria-Bertani) medium was prepared using 2 g NaCl, 2 g peptone from Merck, 1 g yeast extract from Merck and sterile filtered water, with 2 or 0.5% agar-agar respectively. The membrane boxes and the agar medium were autoclaved in a Certoclav Labor-autoklav for 20 minutes. Agar medium was poured into the boxes to a height that left at least 2 mm of the membrane above the surface. It was important that the agar levels on both sides of the membrane

were equal in height. A lid was put on top of the boxes meanwhile the agar set. They were then dried in an oven at 50°C for 15 min.

The *P. aeruginosa* and *S. aureus* strains used in this study are listed in Table 1. Overnight (ON) cultures, grown at 37°C with shaking (200 rpm), were diluted 10 times with LB medium. The diluted cultures were used to make spot cultures in the membrane boxes, 5 μl on 2% agar, and 3 μl on 0.5% agar. The different single and double membrane box setups are listed in Table 2 and 3, respectively. The spot cultures were generally put at a distance from the membrane to avoid direct contact and ease the observation of the culture morphology. When the spot cultures were dry, the membrane boxes were placed in a closed container where a soaked paper generated a humid environment protecting from dehydration. The membrane box setups were incubated at 37°C for 2-3 days.

Table 1: Bacterial strains used in this study.

Bacterial strain	Relevant genotype description	Reference of source
P. aeruginosa* DK2-*Gfp	Strain P24M2-2003 tagged with $P_{rrnB\ P1}$-*gfpAGA*	(4)
***P. aeruginosa* PaO1**	Wild type reference strain	(51)
***P. aeruginosa* Tn1E8**	Mutant in *pqsB* unable to produce several quinolones	(4)
***S. aureus* JE2**	Wild type	(52)

Table 2: Summary of the single membrane box setups.

Media	Bacterium	Membrane	Bacterium
LB 2%	*S.a* JE2	Millipore 220	*P.a* DK2-*Gfp* /PaO1
LB 2%	*S.a* JE2	Millipore 450	*P.a* DK2-*Gfp* /PaO1
LB 2%	*S.a* JE2	Nano	*P.a* DK2-*Gfp* /PaO1
LB 2%	*S.a* JE2	Non-porous 1,2-PB	*P.a* DK2-*Gfp*
LB 2%	*S.a* JE2	Nano non-hydrophilized	*P.a* DK2-*Gfp*

Table 3: Summary of the double membrane box setups, the same type of membrane was used on both sides of the water phase.

Media	Bacterium	Membrane	Water phase	Bacterium
LB 0.5%	*S.a* JE2	Millipore 220	H_2O	*P.a* DK2-*Gfp* /PaO1/ *P.a* Tn1E8
LB 0.5%	*S.a* JE2	Millipore 450	H_2O	*P.a* DK2-*Gfp* /PaO1/ *P.a* Tn1E8
LB 2%	*S.a* JE2	Nano	H_2O	*P.a* DK2-*Gfp* /PaO1
LB 2%	*P.a* DK2-*Gfp*	Nano	Amino acids	*P.a* DK2-*Gfp*

The nanoporous membranes were reusable. To remove residues of agar and bacteria they were rinsed in boiling water and ethanol. The Millipore membranes were always replaced by new after each growth experiment, since they cannot withstand more than one autoclave cycle without detrimental effects.

In the case where double-membrane systems were used, 200 μl sterile filtered water was pipetted into the column between the membranes, once the spot cultures were dry, to the same height as the agar medium. The water phase was in some cases replaced by a reagent solution as for example Casamino acids. After one day of incubation the water level was verified and, if needed, more was added to be in level with the agar, and then incubated for another day.

3.4.1 Sample preparation

After incubation the water phases were collected with a syringe and stored in an eppendorf® tube at -22°C for further analysis. For UV-Vis the samples were used without further treatment. For MALDI-TOF MS the samples were diluted 1:1 with ethyl acetate and mixed thoroughly by vortexing, and left for two hours, the same way as with the agar extracts, see section below. The samples were stored at -22°C until MALDI-TOF MS analysis was performed.

3.4.2 Agar extracts

From the petri dishes, pieces of agar were cut out in proximity to the spot cultures in order to examine the secreted molecules. Each piece was placed in an eppendorf tube where 100 μl of ethyl acetate was added, and then thoroughly vortexed. The samples were mixed several times during two hours and then centrifuged to get rid of the agar. The supernatant was collected and stored at -22°C until MALDI-TOF MS analysis was performed.

3.5 Analysis of bacterial growth, phenotypes and signal molecules

3.5.1 Bacterial growth and phenotypes

The bacterial growth and phenotypes in the membrane boxes were analyzed visually and compared with the controls.

3.5.2 Detection of bacterial signalling molecules in the water phases

3.5.2.1 UV-Vis

A Shimadzu 2600 tandem UV-Vis spectrometer with Quantum Spectra as software was used to analyze the absorption in the water phase samples. Suprasil® quartz precision cells from Hellma, only requiring 80 μl sample, were used in order to minimize the sample volumes. Bacterial signalling molecules as amino acids have their typical absorbance spectra between 200-300 nm and absorb very little above 300 nm (46). This is why cuvettes made of quartz had to be used, since it is the only material that is transparent at such short wavelengths.

First, a background scan was performed with MilliQ water in both cuvettes. One cuvette was always kept as reference and the other one was subject to the different samples with rigorous cleaning in between. In order to do measurements well below the saturation level of the transmittance detector, the samples were diluted.

3.5.2.2 MALDI-TOF MS

An α-cyano-4-hydroxycinnamic acid (CHCA) [Sigma Aldrich] matrix in aceto nitrile was prepared according to Gogichaeva and Alterman's protocol for MALDI-TOF MS analysis of amino acids (53). The samples were mixed with matrix in 1:1 ratio and 1 μl was pipetted onto the MALDI-TOF sample array. A Bruker Autoflex speed TOF/TOF was used in positive ion detection mode, with 60-80% laser power, a laser trigger frequency of 200 Hz, 7x detector gain and with 4000 shots per spectrum were collected. The spectra were acquired using the software flexControl and analyzed in flexAnalysis.

4 Results

4.1 Membrane characterization

The membranes were characterized before use in the bacterial growth setups to examine their properties and control their suitability for the experiment.

4.1.1 Scanning electron microscopy

The SEM micrograph in Figure 23 shows the bulk of a block copolymer membrane in the (211) projection of the gyroid morphology. This projection is also known as 'knitting pattern' due to its characteristic appearance. The image is not sharp due to charging.

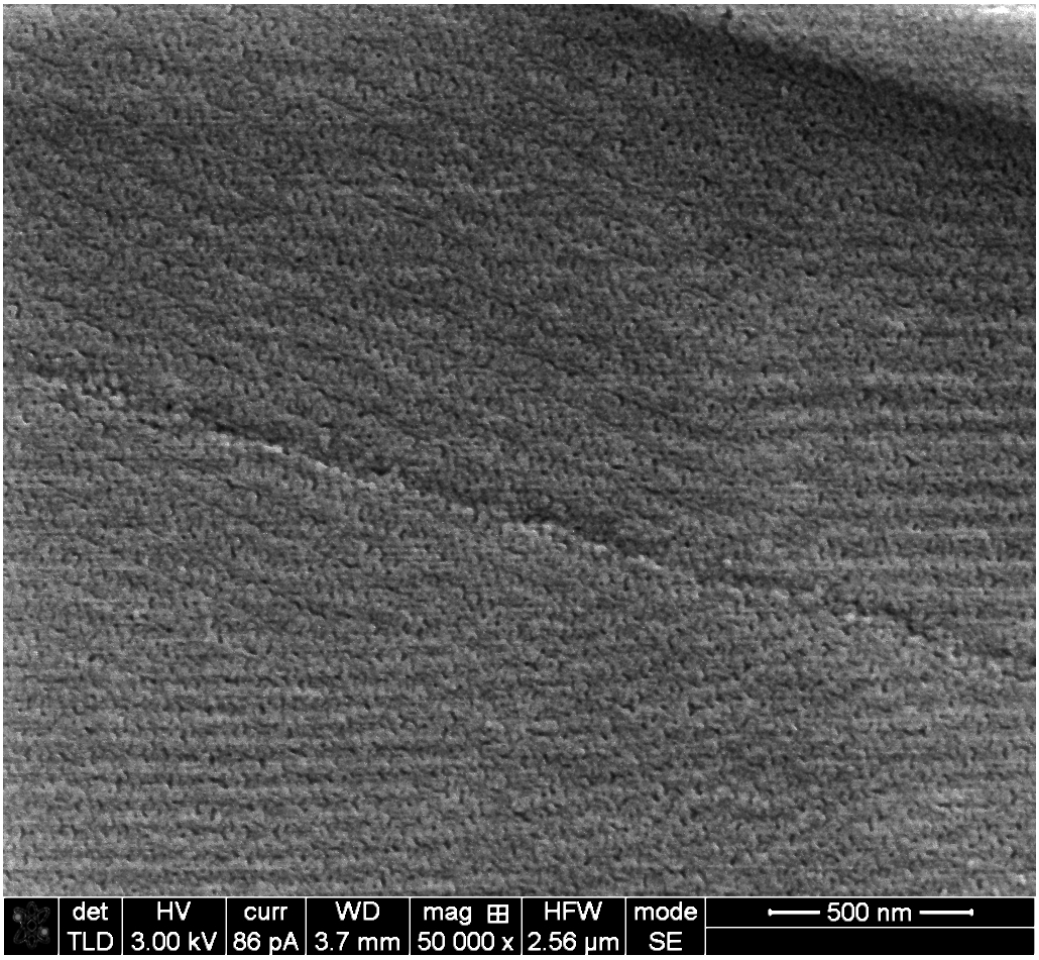

Figure 23: SEM micrograph of the bulk in a membrane, showing gyroid morphology in form of a knitting pattern (211). The image is not sharp due to charging.

4.1.2 Transmission electron microscopy

The TEM micrograph in Figure 24 shows the cross-section of the surface and the bulk in a block copolymer membrane. The (111) projection of the gyroid morphology also known as 'wagon wheel' is clearly shown. The structure continues throughout the sample, confirming an open and porous structure.

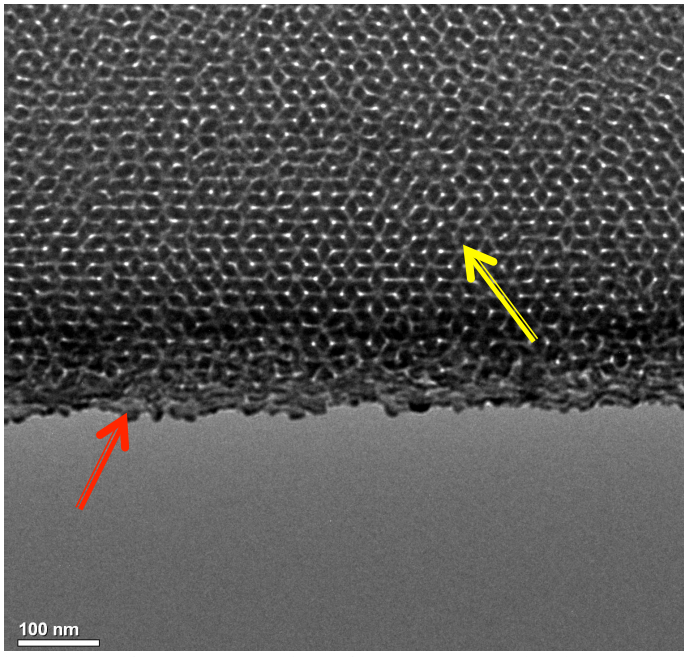

Figure 24: TEM micrograph of the cross-section of a membrane, clearly showing gyroid morphology in form of the wagon wheel (111) projection. The red arrow indicates the membrane surface, and the yellow arrow indicates the bulk.

4.1.3 FT-IR

The FT-IR spectra in Figure 25, show the composition of the membrane after the different fabrication steps. It can be seen how absorptions peaks appear and disappear in the course of modifications. The non-etched membrane is represented in the red spectrum and has intense peaks at 794, 1014, 1086, 1259 cm^{-1}, corresponding to PDMS. After etching of PDMS, the black spectrum shows that these peaks disappear as the Si-O repeating units in the block copolymer have been removed. The blue spectrum shows a hydrophilized membrane where absorption peaks appear at 1 050 and 1 220 cm^{-1} because of the symmetric and asymmetric stretching in S=O from the sulfonic groups of MESNA (27).

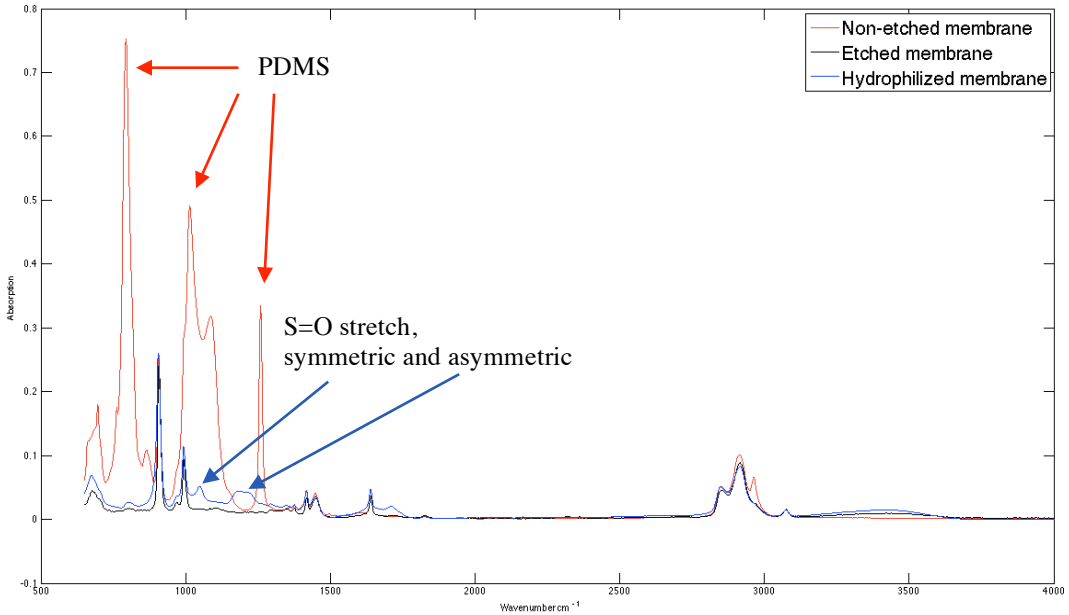

Figure 25: FT-IR spectra before modification (non-etched) and after etching and hydrophilization.

4.1.4 Contact angle

The contact angle measurements show the difference between the surface of a hydrophilized and a hydrophobic membrane, Figure 26. Both measurements were performed on the glass-side of the membrane. The hydrophobic sample has a CA of 98±3° and the hydrophilic a CA of 32±2°. These results confirm a successful hydrophilization.

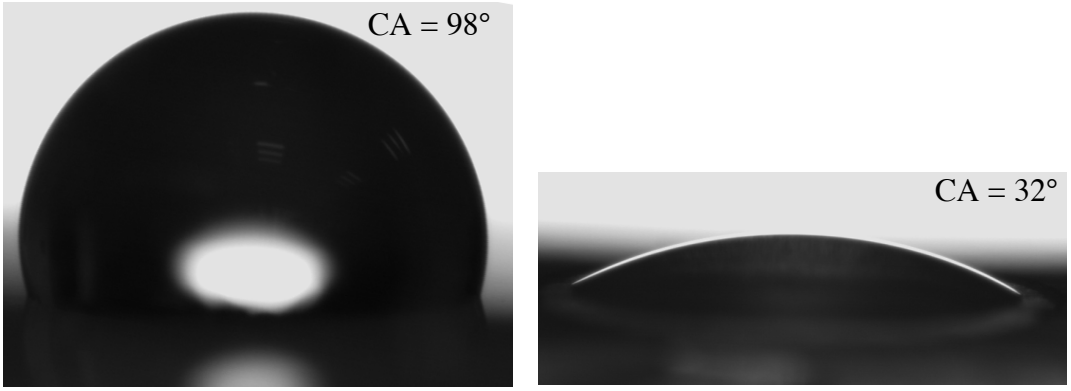

Figure 26: Contact angle measurements on the glass side of a membrane before and after hydrophilization.

4.1.5 Sink test

Depending on the nature of the membranes they had different sinking patterns. In the sink test with methanol the porosity was proved as the membranes sunk without external influence after around 2 seconds. For the hydrophilized membranes that were put in water the sinking was slower. They stayed at the surface until they were completely filled with water, and an easy push was required to make them sink due to surface tension. These results confirm a porous structure and a successful hydrophilization of the membranes. A non-hydrophilized membrane that is put in water floats up to the surface no matter how long time it is held under water.

4.1.6 Permeability test

In Figure 27 the result from a nanoporous membrane can be seen. The membrane got completely pink in just a few seconds and the side with phenolphthalein was colored pink after 30 minutes. This result indicates that the membranes were permeable to small molecules as hydroxide ions.

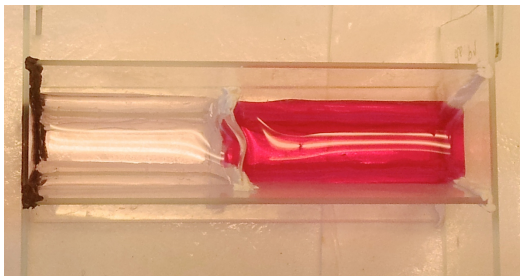

Figure 27: Permeability test carried out in a sandwich membrane setup. The phenolphthalein side had turned completely pink after 30 minutes.

4.2 *P. aeruginosa* – *S. aureus* interactions

The goal of our project was to see if any effect of bacterial interaction could be detected when a permeable membrane separated the two bacterial colonies.
The effects studied (see Figure 3) were:

- A zone with induced growth in *P. aeruginosa*, with decreased autolysis and supressed iridescent metallic sheen coverage, which will be referred to as the GZI (growth zone induced) phenotype.
- An induced yellow pigmentation in *S. aureus*, which will be referred to as YPI (yellow pigment induced) phenotype.

We make the grammatical decision to refer to the compounds that causes the GZI and YPI phenotypes as single molecules. Still, we are well aware that these effects could be caused by several compounds and maybe not only single molecules.

In addition to the GZI and YPI phenotypes, two other phenotypes were frequently observed.

- A zone in *P. aeruginosa* DK2 with a smooth surface from decreased autolysis, and an increased metallic sheen coverage, which will be referred to as the FZ (flat zone) phenotype, see Figure 30B
- Inhibition of *S. aureus* resulting in a transparent zone, see Figure 1 in appendix 1.

4.2.1 Bacterial growth and phenotypes in the single membrane setup

The results from the single membrane setup experiments are summarized in Table 4, where the results from the reference experiments in petri dishes are included for comparison.

Table 4: Phenotypes of *P. aeruginosa* and *S. aureus* after interactions of *S. aureus* with *P. aeruginosa* DK2-*Gfp*, PaO1 and Tn1E8.
–, None; +, low; ++, medium; +++ high; induction.

Setup	*Pseudomonas* strain	FZ	GZI	YPI	Inhibition of *S. aureus*	Figure reference
Milli 220	*P.a* DK2-*Gfp*	+	-	++	-	28A
Milli 220	PaO1	-	-	+	+	28C
Milli 450	*P.a* DK2-*Gfp*	+	-	++	-	28B
Milli 450	PaO1	-	-	+	++	28D
Nano	*P.a* DK2-*Gfp*	+	-	-	-	29A,B
Nano	PaO1	-	-	-	-	29C
Non-porous 1,2-PB	*P.a* DK2-*Gfp*	+	-	-	-	Data not shown
Nano - hydrophobic	*P.a* DK2-*Gfp*	+	-	-	-	Data not shown
Petri dish (reference)						
Petri dish	*P.a* DK2-*Gfp*	-	+	+++	-	Appendix 1.2
Petri dish	PaO1	-	-	+	+++	Appendix 1.1
Petri dish	*P.a* Tn1E8	-	-	-	-	Appendix 1.3

In Figure 28 it is shown that *P. aeruginosa* has affected *S. aureus* through the Millipore membranes by inducing yellow pigment production. In Figure 28A and B, the cultures that are in contact with the membranes express a strong yellow color. The color is more pronounced in the setup with Millipore 450 nm (Figure 28B) than 220 nm (Figure 28A). The *P. aeruginosa* DK2 colonies have a flat zone with decreased autolysis and increased metallic sheen closest to the membrane. When co-cultured without a membrane, PaO1 would kill *S. aureus* but as we can see in Figure 28C and D this has not happened. *S. aureus* is inhibited closest to the membrane (transparent colony) and slightly yellow at the opposite side of the culture. The pictures in Figure 28 were taken after two days of incubation.

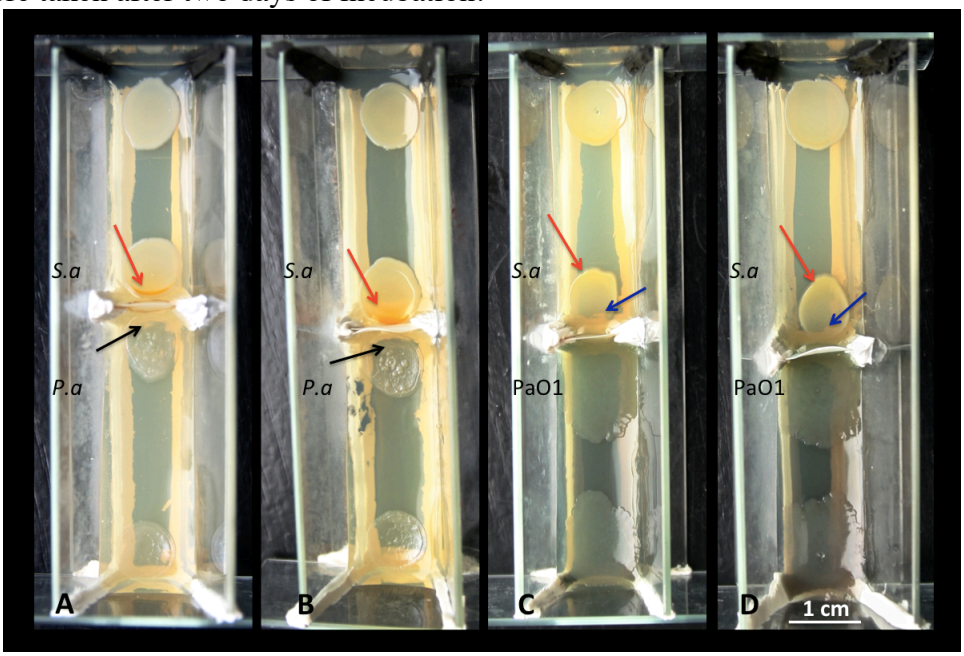

Figure 28: Single Millipore membrane setups, A) and C) having 220 nm pores and B) and D) 450 nm pores. In A) and B) there is a yellow pigmentation (red arrows) of the *S. aureus* culture closest to the membrane, while the *P. aeruginosa* DK2 culture shows the FZ phenotype (black arrows). In C) and D) there is a zone of inhibition of *S. aureus* closest to the membrane (blue arrows) and the opposite side of the culture is slightly yellow (red arrows), while PaO1 is unaffected. Grown on 2% LB agar.

In the setup with single nanoporous membranes the YPI molecule from *P. aeruginosa* to *S. aureus* is blocked, resulting in no pigmentation of the *S. aureus* colony closest to the membrane, see Figure 29. In Figure 29A and B there is a flat zone in the *P. aeruginosa* DK2 colony showing decreased autolysis and increased metallic sheen closest to the membrane. The knobby surface that otherwise is characteristic for the *P. aeruginosa* with a mutation in *lasR* is due to autolysis, which makes it possible to believe that the altered *P. aeruginosa* colony morphology in this case is due to growth induction from the *S. aureus* interaction. Together with the growth zone induction, however, suppression of the iridescent metallic sheen coverage should be seen in the *S. aureus* JE2 – *P. aeruginosa* DK2 interaction, which was not the case in the presence of the nanoporous membrane (Figure 29A and B). The smooth surfaces close to the membranes showed predominantly more metallic sheen than the control culture.

The interaction between *P. aeruginosa* PaO1 and *S. aureus* that was observed in the Millipore setup does not appear in the nano membrane setup, as seen in Figure 29C. There is no yellow pigmentation, nor inhibition of *S. aureus* by *P. aeruginosa* PaO1.

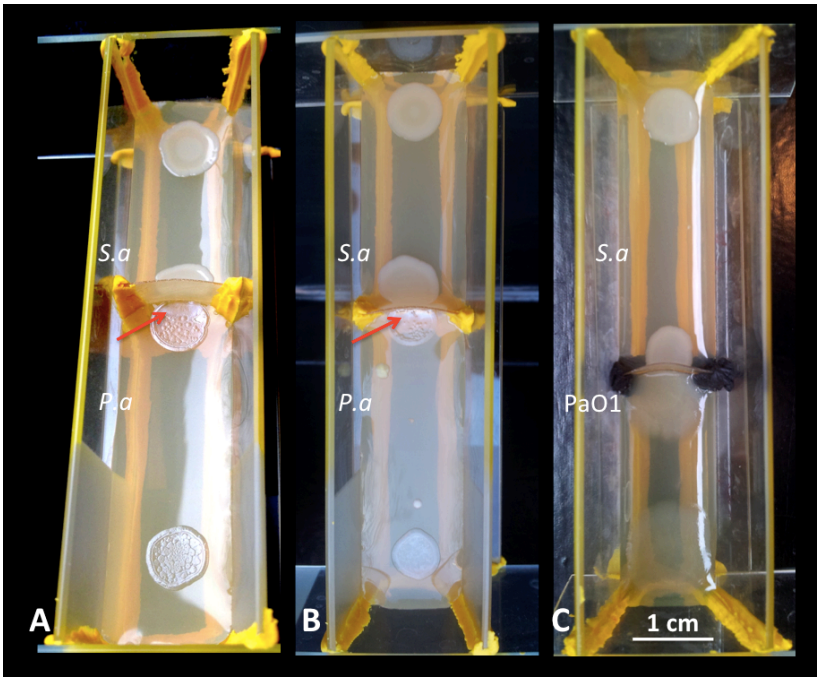

Figure 29: Single nano membrane setup. A) A densely white zone with metallic sheen was observed in the *P. aeruginosa* DK2 colony closest to the membrane (red arrow). B) A flat zone with decreased autolysis and increased metallic sheen is observed in the *P. aeruginosa* DK2 colony (red arrow). C) No interaction is observed. Grown on 2% LB agar.

To verify whether it was the nanoporous membranes or the *S. aureus* that had an effect on the *P.* aeruginosa colony morphology, the same experiment was repeated where the *P. aeruginosa* colonies were not in contact with the membranes. The zone with a smooth surface from decreased autolysis, and with increased metallic sheen coverage was then observed, see Figure 30B. As seen in Figure 30A, the *P. aeruginosa* DK2 colony shows no smooth zone as the one observed in 30B. The colony morphology looks just like the control colony. This shows that there is no clear correlation between membrane impact and colony morphology. The FZ phenotype was also observed when a non-porous or a hydrophobic membrane was used as barrier in the single membrane setup, see Table 4.

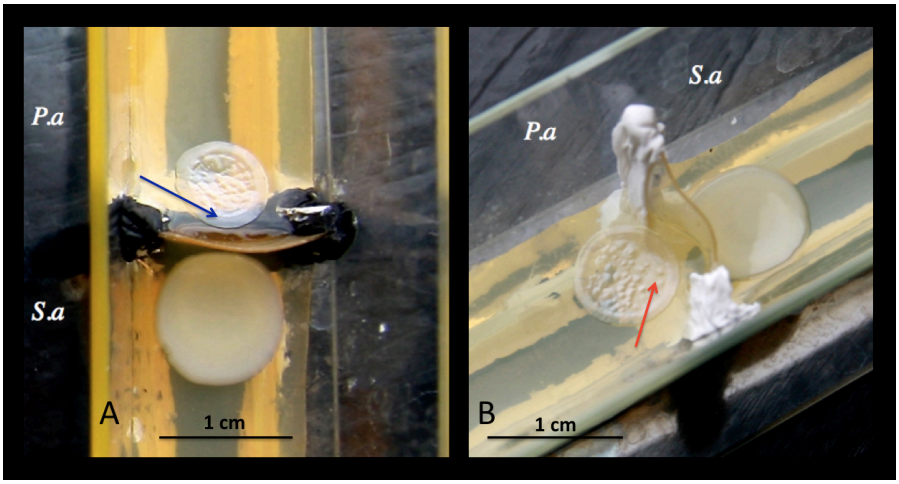

Figure 30: Single nano membrane setups where the *P. aeruginosa* cultures are not in contact with the membrane. A) No effect (blue arrow) from the membrane is observed in the colony morphology of *P. aeruginosa* DK2. B) The red arrow indicates the zone with a smooth surface closest to the membrane. Grown on 2% LB agar.

4.2.2 Bacterial growth and phenotypes in the double membrane setup

The results from the double membrane setup experiments are summarized in Table 5.

Table 5: Phenotypes of *P. aeruginosa* and *S. aureus* after interactions of *S. aureus* with *P. aeruginosa* DK2 Gfp, PaO1 and Tn1E8.
–, None; +, low; ++, medium; +++ high; induction.

Setup	***Pseudomonas* strain**	**FZ**	**GZI**	**YPI**	**Inhibition of *S. aureus***	**Figure reference**
Milli-milli 220 (water)	*P.a* DK2 *Gfp*	+	-	+	-	31A
Milli-milli 220 (water)	PaO1	-	-	(½) +	+	31B
Milli-milli 220 (water)	*P.a* Tn1E8	-	-	-	-	31C
Milli-milli 450 (water)	*P.a* DK2 *Gfp*	+	-	+	-	Data not shown
Milli-milli 450 (water)	PaO1	-	-	(½) +	+	Data not shown
Milli-milli 450 (water)	*P.a* Tn1E8	-	-	-	-	Data not shown
Nano-nano (water)	*P.a* DK2 *Gfp*	+	-	-	-	Data not shown
Nano-nano (water)	PaO1	-	-	-	-	Data not shown
Nano-nano (amino acids, no S. aureus)	*P.a* DK2 *Gfp*	+	-	-	-	Data not shown

We further developed a setup with two membranes, for extraction and detection of signalling molecules. In this setup, the signalling molecules had to diffuse through a water phase in between the membranes to reach the other bacterial colony. The YPI phenotype was observed in *S. aureus* JE2 in the milli-milli membrane setup when semi-solid LB 0.5% agar was used as growth medium, see Figure 31A. In Figure 31A *S. aureus* is co-cultured with *P. aeruginosa* DK2 (which shows a completely different colony morphology when grown on semi-solid agar compared to solid LB 2% agar). In the *S. aureus – P. aeruginosa* PaO1 interaction, shown in Figure 31B, the YPI phenotype and the inhibition of *S. aureus* is observed, but less significant than in the single membrane setup. In Figure 31C, the *S. aureus – P. aeruginosa* Tn1E8 interaction is shown and no change in morphology is observed, as expected.

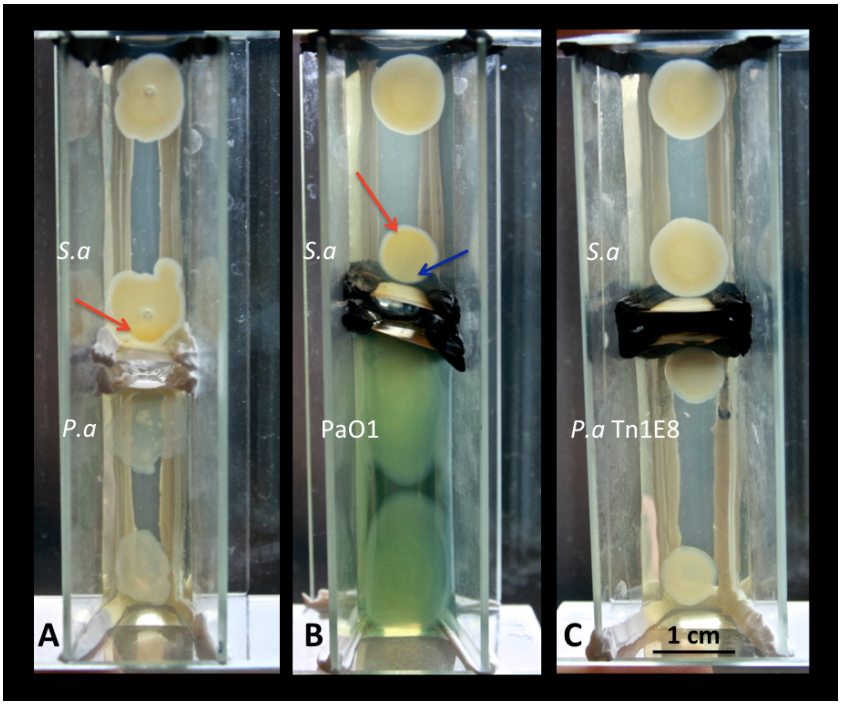

Figure 31: Double membrane setup with Millipore 220 nm. In A) there is a yellow pigmentation of *S. aureus* closest to the membrane, indicated by red arrow, while *P. aeruginosa* DK2 is unaffected. In B) the YPI phenotype (red arrow) and inhibition (blue arrow) of *S. aureus* by *P. aeruginosa* PaO1 is observed. In D) no change in morphology is observed on either colony, as expected when *P. aeruginosa* Tn1E8 is used. Grown on LB 0.5% agar.

In the double membrane setup with nanoporous membranes no YPI phenotype on *S. aureus* was observed, which was in line with the results from the single nanoporous membrane setups. The FZ phenotype in *P. aeruginosa* DK2 was however observed.
In addition, the FZ phenotype was observed in the experiment with *P. aeruginosa* DK2 on both sides of the water phase and with a solution of Casamino acids (0.2 and 2%) introduced in the water phase. The GZI phenotype was not observed.

4.2.3 Detection of bacterial signalling molecules in the water phases

4.2.3.1 UV-Vis

Figure 32 shows the result from the UV-Vis analysis of the water phases. It is clearly visible that the water phase from the *S. aureus* JE2 – *P. aeruginosa* DK2 interaction (pink spectrum) and the agar background (blue spectrum) have a similar appearance, rendering the detection of signalling molecules impossible. The (green) spectrum from the water phase from the *S. aureus* JE2 – PaO1 interaction has two absorbance peaks, at 313 and 367 nm, not visible elsewhere. The peaks were compared with earlier results (54), and the presence of the pigment pyocyanin typical for *P. aeruginosa* was confirmed.

For comparison the spectrums of 100 µM HHQ (red) and 2% Casamino acids (black) were measured. These solutions of pure compounds have a very low absorbance in comparison to the water phases, even at high concentrations, diminishing the chances to detected them as signal molecules in a water phase sample.

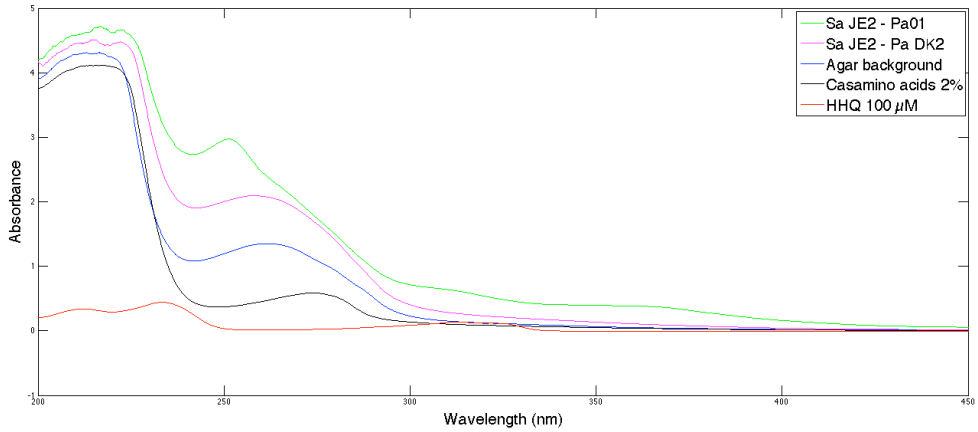

Figure 32: UV-Vis spectrum showing the absorbance of the water phases from the *S. aureus* JE2 – PaO1 and the *S. aureus* JE2 – *P. aeruginosa* DK2 interactions. For comparison the spectrums of agar, Casamino acids and HHQ are included.

4.2.3.2 MALDI-TOF MS

The spectra from the MALDI-TOF MS analysis of the samples from the Millipore 220 and 450 double membrane setups are presented in Figures 33-35. In all spectra the matrix and the LB medium are contributing to several peaks, rendering the search for the signal molecules more complicated. To ease the search for signal molecules as quinolones, an agar extract sample from between a *P. aeruginosa* Tn1E8 and a *S. aureus* JE2 culture was used as reference. *P. aeruginosa* Tn1E8 is unable to produce several quinolones and will thus facilitate the detection of these molecules. However, *S. aureus* JE2 is used in both the sample and the reference setup, leading to the potential coverage of signals from its secretion.

The MADLI-TOF MS spectra were screened for compounds that differed from the reference. Especially, peaks at 244, 258, 270, 272 and 298 *m/z* were searched for, since they have been reported to be signal molecules from *P. aeruginosa* DK2 in interaction with *S. aureus* (36). The results are summarized in Table 6.

Table 6: Water phases after interactions of *S. aureus* with *P. aeruginosa* DK2-*Gfp*, PaO1 and Tn1E8. –, No; +, Yes.

Setup	*Pseudomonas* strain	m/z 235	*m/z* 244	*m/z* 258	*m/z* 270	*m/z* 272	*m/z* 298
Milli-milli 220 (water), Figure 33	*P.a* DK2-*Gfp*	+	+	-	-	-	-
Milli-milli 450 (water), Figure 34	*P.a* DK2-*Gfp*	+	-	-	+	-	-
Milli-milli 450 (water), Figure 35	PaO1	+	+	+	+	+	+
Agar extract (Appendix 1.3)	*P.a* Tn1E8	+	-	-	-	-	-

Figure 33 presents the analysis of the water phase from a Millipore 220 double membrane system with *P. aeruginosa* DK2 and *S. aureus* JE2. The peaks at 235 and 244 *m/z* are not present in the reference, indicating the existence of signal molecules as quinolones in the samples.

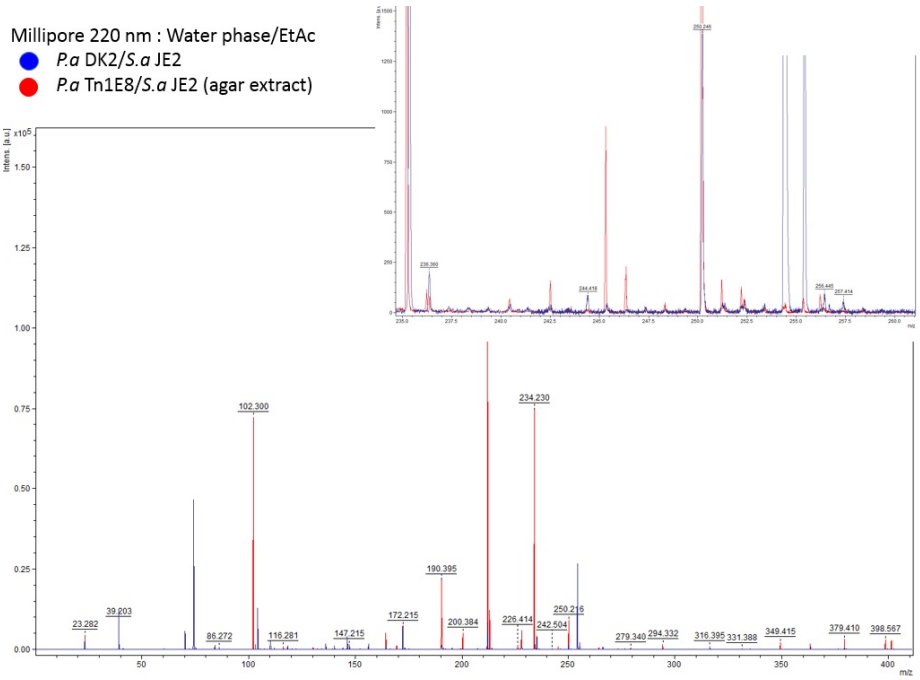

Figure 33: MALDI-TOF spectrum from the analysis of the water phase (with additional EtAc) from a Millipore 220 double membrane system with *P. aeruginosa* DK2 and *S. aureus* JE2. The reference in red is an agar extract from between a *P. aeruginosa* Tn1E8 and a *S. aureus* JE2 culture. The inset is a close-up of the peaks 235 and 244 *m/z*. For large view of spectra see Appendix 2.1-2.

Figure 34 presents the results from the analysis of the water phase from a Millipore 450 nm double membrane system with *P. aeruginosa* DK2 and *S. aureus* JE2. The peaks at *m/z* 235 and 270 are not present in the reference, and the one at *m/z* 270 correlate with one of the reported (36), (55) quinolones from *P. aeruginosa*.

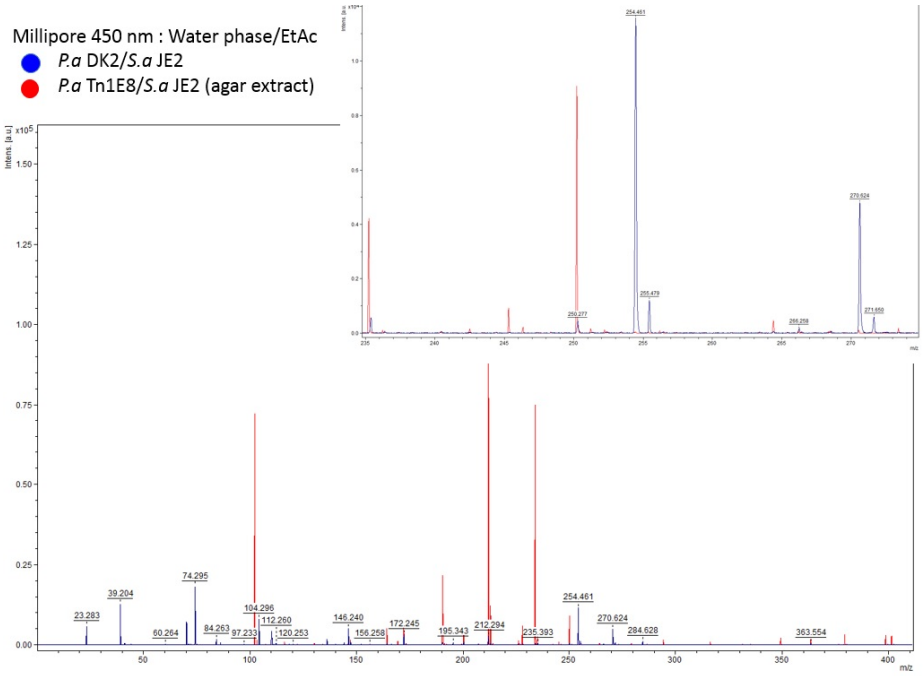

Figure 34: MALDI-TOF spectrum from the analysis of the water phase (with additional EtAc) from a Millipore 450 nm double membrane system with *P. aeruginosa* DK2 and *S. aureus* JE2. The reference in red is an agar extract from between a *P. aeruginosa* Tn1E8 and a *S. aureus* JE2 culture. The inset is a close-up of the peaks 235 and 270 *m/z*. For large view of spectra see Appendix 2.3-4.

Figure 35 presents the result from the analysis of the water phase from a Millipore 220 nm double membrane system with *P. aeruginosa* PaO1 and *S. aureus* JE2. In this sample several interesting peaks were found; 235, 244, 258, 270, 272 and 298 *m/z*.

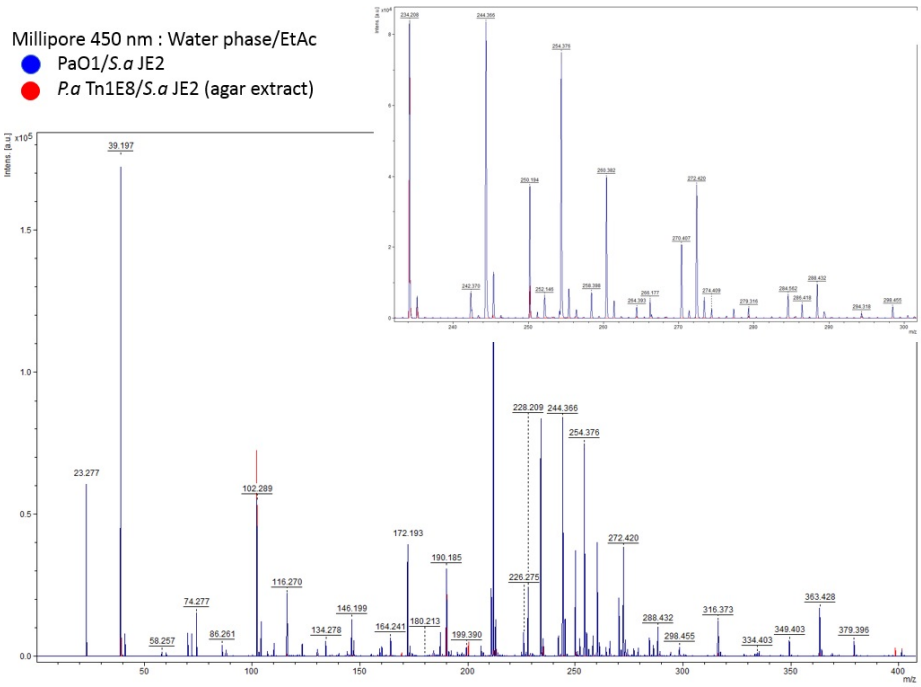

Figure 35: MALDI-TOF spectrum from the analysis of the water phase (with additional EtAc) from a Millipore 450 nm double membrane system with PaO1 and *S. aureus* JE2. The reference in red is an agar extract from between a *P. aeruginosa* Tn1E8 and a *S. aureus* JE2 culture. The inset is a close-up of the peaks 235, 244, 258, 270, 272 and 298 *m/z*. For large view of spectra see Appendix 2.5-6.

5 Discussion

5.1 The membrane box setup

The aim of this project was primarily to investigate the possibility of using membrane box setup for the study and analysis of *P. aeruginosa – S. aureus* interactions. To our knowledge such a system have never been reported before and we can conclude that there is still a long way to go. The growth chamber design worked satisfactory with respect to the experiments, but it was very time consuming to exchange the Millipore membranes after each experiment.

Some difficulties were experienced with the methods used to analyze bacterial interactions in our membrane box setup. Visual observation of the colonies was not completely reliable, since new factors, e.g. a highly porous and hydrophilized surface and the presence of the Sugru clay, for the bacteria to adapt to were introduced. An experienced person that is familiar with the morphologies of the colonies is therefore crucial for this analysis method to be reliable. Here, fluorescence microscopy would be a suitable supplement (as described by Charlotte et al. (4)). We used a *Gfp*-tagged *P. aeruginosa* DK2 strain in our setup, however we experienced that the LB medium was highly fluorescent itself, and therefore fluorescence microscopy was not applicable.

The membrane box setup has several advantages for studies of bacterial interactions, particularly the ability to perform size exclusion by using membranes with several different pore sizes. We restricted this work to three different pore sizes, but more should be utilized in order to gain as much knowledge as possible about the GZI and YPI signal molecules. Another important advantage is that the setup allows the bacteria to be physically separated, which can be used to investigate if the interaction only takes place when the bacteria are in contact. A powerful property of the double membrane setup is that bacterial interactions, induced by signal molecules with sufficient concentration and diffusion capacity, can act across a water phase. This facilitates the analysis of the signalling molecules in the water phase, by for example MALDI-TOF MS.

Overall, the membrane box setup needs a lot of optimization in order to be a versatile tool in bacterial interaction analysis. There are some important drawbacks that have to be taken into account. The membrane box setup is unfavorable to use when the signal molecules only are present at low concentrations, due to the dominant signals from the growth media in MALDI-TOF MS and UV-Vis analysis. Improvements might be achieved by using a thinner membrane, a smaller colony-to-colony distance, and lowered water phase volume. Optimization of incubation time for the specific bacterial interaction is as well a means to capture the highest possible concentration of signal molecules. Although, low concentrations of signal molecules in the water phase and interfering signals from growth media will probably continue to be an issue. Another aspect is that the effect of interaction should preferably be easy to detect, as in this setup, where visual observation was the GZI and the YPI phenotypes were the main analysis method.

5.2 Membranes

The membranes that were used fulfilled their purposes, since size exclusion of the YPI molecule was achieved between the 10 nm and the 220 nm pores. The properties of the membranes differ in several aspects apart from the pore size. The Millipore membranes are thinner than the nanoporous, which might facilitate the diffusion through the membranes. By comparing the SEM micrograph of the Millipore membrane (Figure 18) and the TEM micrograph of the nanoporous membrane (Figure 24) we can conclude that the pore size distribution is larger in the Millipore membrane. The regularity in the TEM micrograph of the nanoporous membrane indicates that it is highly ordered with a very narrow pore size distribution. This could be an advantage when more specific size exclusion is desired. The reusability of the nanoporous membranes saved a lot of time as they did not need to be exchanged as the Millipore membranes. However, the Millipore membranes were commercially available and thus standardized with very small variations in measurements compare to the fabricated nanoporous membranes.

5.2.1 Block copolymer based membranes

5.2.1.1 Membrane porosity and permeability

The membrane fabrication was developed during the project. The most prominent change was to cross-link the membrane film with both surfaces in contact with glass, instead of one in contact with air and one with glass. Hereby, membranes with a skin-

layered air-side were avoided. The skin-layer is suggested to have a thickness of 30 nm after the etching of PDMS (7), and a sandpaper can be used to remove it. The change from the air-side method with additional sandpapering to the sandwich method increased the permeability of the membranes significantly. The membranes with a sandpapered air-side got pink spots within 30 minutes in the permeability test, which proved that the KOH and phenolphthalein met inside the pores, meanwhile the sandwiched membranes turned completely pink already within two minutes. After 30 minutes, the side with phenolphthalein was entirely pink, indicating that small molecules as hydroxide ions more easily diffused through the sandwiched membrane.

The membrane surfaces were examined by SEM to observe the difference of the air-side and glass-side structures, and to determine if the sandpapering was a suitable method for the skin-layer removal. Even though the samples were sputtered with gold and copper tape was used to ground the samples on the sample holders, we experienced big charging effects and the micrographs were very blurred. No gyroid structure was detected on the surface of any sample, most probably because of poor imaging conditions. Therefore no correct interpretations could be made based on these results. Attempts to reduce the charging effect were made. An extra thick layer of gold was sputtered on the samples, but this resulted in closed and covered pores and all that could be distinguished was a gold surface.

Instead, TEM was used to characterize the surface porosity. Thin microtomed slices from the membrane cross-section were analyzed. The micrograph in Figure 24, confirms the presence of an open and porous structure both in the bulk and at the surface. This result directly indicates that the block copolymer membranes were permeable and functioning as expected.

5.2.1.2 Thickness uniformity and cross-linking degree

The wanted thickness of the membranes was determined already in the fabrication step by calculating the amount of polymer that was dissolved and used for film casting. However, during the drying process the polymer tended to cumulate at the edges of the petri dish, resulting in a very uneven membrane thickness. The thinnest parts in the middle were sometimes down to 100 μm and not 300 μm as they should have been. The thickest edges were cut away and the most uniform parts close to 300 μm were the ones we used.

The difference in thickness could be responsible for a difference in cross-linking degree across the membrane film. A difference in cross-linking degree would implicate that there is a difference in free-hanging double bond concentration that can interact with the surrounding media. It was suggested that this could be a reason for one of the big problems that was encountered in the project; when the membranes were put into the etching solution, they bent and the thinnest parts even curled up to rolls. Non-flat membranes are very difficult to work with so several attempts were made to make them flat. A shield was put around the petri dishes during drying to avoid drafts of wind in the fume hood, with some success in fabrication of more evenly thick membranes. A very low relative amount (1% mole) of DCP was used as cross-linker due the fact that the cross-linking is a time-dependent chain reaction. With the objective to get an as even cross-linking degree as possible and a stable structure this relative amount was increased to 1.5% mole, resulting in a slightly harder material but no significant improvement in flatness.

Cross-linking with the sandwich method gave a slightly more uniform film, since spacers determined the thickness. It was, however, difficult to press the top-petri dish in contact with the whole film surface, since some parts were thinner than the spacers. When the sandwiched membranes were put into the etching solution, an interesting observation was made; the parts of the membrane that had been in good contact with the top petri dish stayed much flatter than the other ones. Membranes with a skin-layer have one surface that is covered by PDMS that will react and be removed by TBAF, while a gyroid non-skin surface will provide less reacting PDMS. This could be a reason why membranes with a skin-layer curl up immediately when they come in contact with the etching solution. Membranes with a gyroid structured surface experience the same forces on both sides of the membrane and have therefore no reason to bend.

When the membranes were to be dried after etching, they were first placed in a beaker in the fume hood until all solvent had evaporated. This permitted the membranes to bend freely, and they became unfavourably curved. Therefore, the drying method was changed to drying the membranes between filter papers clamped by glass-slides to force them flat. With this drying method it took longer time for the membranes to dry. Some water seemed to stay in the pores while kept in the drying setup, because the membranes bended slightly when they were taken out from the filter papers.

Overall, the membranes were very sensitive to all wetting- and drying processes, buckled easily and were then unwilling to regress to a flat membrane.

5.2.1.3 Hydrophilization

The hydrophilization method was not changed throughout the process and the same parameters were used. The contact angle measurements showed in a very clear way that the membrane surfaces were successfully hydrophilized. For a non-hydrophilized membrane a difference in the contact angle between a skin surface and a non-skin surface was noticed. The non-skin surface has a porous hydrophobic structure where the capillary forces compel the water, resulting in an increased contact angle. This could have been a good way to determine the surface structure, but our membranes were bent, and the contact angle results therefore difficult to interpret correctly. With flat membranes this method could have given important results.

The sink test was a rapid confirmation of both the porous structure after etching (sink test in methanol), and of the hydrophilization (sink test in water). In the methanol test, the membrane stayed on the surface for a moment until the pores were filled and then sunk fast to the bottom. In the water test, it took longer time for the pores to be filled, and then the high surface tension of water hindered the small and light membrane pieces to sink. A push was required to make the membranes sink. There are several parameters that influence the difference between the two tests. Methanol has a lower density than 1,2-PB, thus less filling of the membrane pores is needed before it sinks. As well, methanol has a lower viscosity and surface tension than water, enabling the membranes to sink without any external force. In water, the membrane has to be completely filled before it sinks, and due to the high viscosity of water, air bubbles are easily trapped in the pores, which delays the sinking.

5.3 Bacterial interaction in the membrane box setup

In this section we will discuss the results from the different membrane setup experiments and analysis, based on the observation of the GZI and YPI phenotypes in *P. aeruginosa* and *S. aureus*, respectively, and the identification of signalling molecules in the water phases.

5.3.1 Observation of the growth zone induced phenotype in P. aeruginosa

In the initial interpretation of the results from the experiments with the nanoporous membranes (Figure 29A), the flat zone next to the membrane in the *P. aeruginosa* colonies was thought to be the GZI phenotype earlier described by Michelsen et al. (4). The observed zone was densely white and showed suppression of autolysis. Molecules that pass through the nanoporous membrane would have a diameter of less than 10 nm and be hydrophilic. This interpretation made us consider that the signal molecules from *S. aureus* could be amino acids. Amino acids are used as signal molecules by many gram-positive bacteria and as described by D'Argenio et al. (15) certain amino acids, as phenylalanine, give an enhanced growth in *lasR* mutated *P. aeruginosa*. Aromatic amino acids can be converted to anthranilic acid via the kyunine pathway. The anthranilic acid is then converted by the enzymes encoded by the *pqsABCDE* operon to produce the quinolone HHQ (Figure 19) (35). Increased production of quinolones, such as HHQ, could be a possible way to induce an increased growth in *P. aeruginosa* DK2 and thereby form a growth zone. In addition, the increased quinolone production in *P. aeruginosa* DK2 could also be responsible for the stress that is imposed on *S. aureus* that causes the YPI phenotype.

The single membrane setups only gave suggestions about the size and hydrophilicity of the GZI and YPI signal molecules from *S. aureus* and *P. aeruginosa*. To be able to identify these molecules the double membrane setup was used. To investigate the impact from amino acids on *P. aeruginosa*, an experiment with the nano-nano double membrane setup was performed, where water phases containing 0.2% or 2% Casamino acids solutions were used. The *P. aeruginosa* DK2 colony morphology did not alter from what had been observed in the single membrane setups and the same flat phenotype with supressed autolysis was later observed in the *P. aeruginosa* colonies in the Millipore setup.

After several repetitions of the single membrane setup experiments, earlier presumptions were questioned. The flat surface next to the membrane lacked zones of autolysis, but had a distinct iridescent metallic sheen coverage. The *P. aeruginosa* GZI phenotype presented by Michelsen et al. (4) shows a suppression of metallic sheen coverage by the signal molecule from *S. aureus*. The growth zone should also be densely white (Figure 3) (4), which was not detected more than once in our setup (Figure 29A). It is therefore unlikely that the GZI molecules from *S. aureus* pass through neither the Millipore nor the nanoporous membranes. The increased metallic sheen coverage in *P. aeruginosa* might instead be the result of a change in the ratio of expressed AQs, making the HHQ more dominant.

Two explanations were found for the emergence of a flat zone with iridescent metallic sheen coverage (increased HHQ expression) in the *P. aeruginosa* colonies. The zone could result from the influence of small hydrophilic signal molecules from *S. aureus*, whose impact are insignificant when *S. aureus* and *P. aeruginosa* are co-cultured

without a membrane. When the GZI molecules are unable to affect *P. aeruginosa*, the influences of other molecules are detectable. For example it could be peptidoglycans as GlcNAc shed from the cell wall of *S. aureus* that causes this zone. It has earlier been reported that such peptidoglycans enhance the production of virulence factors in *P. aeruginosa* through an induction of *pqsA* (16). This effect has not been studied with our *P. aeruginosa – S. aureus* interaction, and therefore the influence on the *P. aeruginosa* DK2 colony morphology observed in our setup needs to be further analyzed.

The other explanation is based on the possible influence of the membrane itself or of the Sugru clay on the *P. aeruginosa* culture. To investigate the impact of the membrane, *P. aeruginosa* was cultured in contact with a non-porous, a hydrophobic and a hydrophilized membrane respectively. In all setups the flat area with metallic sheen coverage appeared. Even when *P. aeruginosa* was cultured with a distance to the membrane the characteristic area was observed (Figure 30B). To investigate the impact of having Sugru close to the bacterial colonies, a membrane-formed barrier made of the silicon clay was mounted in the box-setup. We could conclude that this setup also resulted in a flat area with iridescent metallic sheen where the bacteria and the clay were in contact (data not shown). These divergent results make it difficult to interpret a complete explanation for the emergence of this zone. However, it is most likely that both the membrane and the Sugru stress *P. aeruginosa* DK2. In contrast, the *S. aureus* colony morphology is unaffected by the presence of the clay and any membrane. This is probably due to the fact that *S. aureus* JE2 is a wild type strain meanwhile the *P. aeruginosa* DK2 strain is highly mutated from years of adaption to the environment of the lungs of a CF patient (4), (13), (15). *P. aeruginosa* DK2 is easily stressed by the new and unfamiliar environment which results in change of morphology.

Another aspect that could have influenced the GZI phenotype in *P. aeruginosa* is the choice of growth media components. In the study by Michelsen et al. (4), where the growth zone is very clearly observed (Figure 3), agar from Sigma Aldrich was used in the LB medium. In our study, a cheaper and a less well-defined agar from Merck was used, and it is possible that there are compounds in this product that affect *P. aeruginosa* in a way that the growth zone is less pronounced, and hard to detect in our setup. In another study by Michelsen (36) Tryptic Soy Broth (TSB) with 1.2% agar (=TSA) from Sigma Aldrich was used, also with successful results. To investigate if another growth medium could change the outcome of the experiment, membrane box experiments with 1.2% TSA were performed. However, no agar from Sigma Aldrich was available so the same agar as in the LB medium was used, but in a lower amount. This experiment resulted in a slightly different colony morphology than when grown on LB agar, but still no characteristic *P. aeruginosa* GZI phenotype could be observed. Therefore, LB was further used to keep consistency in the experiments.

5.3.2 Observation of the yellow pigment induced phenotype in S. aureus

The results from the nanoporous membrane setup clearly showed that the YPI molecule from *P. aeruginosa* was blocked by the membrane (Figure 29A and B). The *S. aureus* phenotype was not altered even after longer times of incubation in the nanoporous membrane setup. A hindered passage of the YPI molecule would

implicate that the molecules are hydrophobic and/or larger than the pore size of 10 nm. However, signal molecules tend to be small in size. Therefore another explanation that implies vesicle transportation was considered. Hydrophobic molecules can be secreted in vesicles to enable their transportation in hydrophilic media. Vesicles usually have a diameter between 50-250 nm (39), which would explain why the YPI molecule cannot pass the nanoporous membrane.

In the Millipore setup we saw the YPI phenotype in the *S. aureus* colony closest to the membrane (Figure 28A and B). As the affected area is next to the membrane these results strongly indicate that the YPI molecule from *P. aeruginosa* DK2, that affects *S. aureus* when they are co-colonized without a barrier, also manage to pass through the membrane. The same Millipore membrane setup was tried with *S. aureus* and the *P. aeruginosa* reference strain, PaO1. As mentioned before PaO1 kills *S. aureus* when co-cultured, but in this setup *S. aureus* was instead only somewhat inhibited closest to the membrane, and showed indication of the YPI phenotype in the other end of the colony (Figure 28C and D). From this we conclude that both *P. aeruginosa* PaO1 and DK2 have the ability to induce yellow pigmentation in *S. aureus*. However, the function of Millipore 450 nm as barrier was questioned as PaO1 managed to go through the membrane after more than 3 days of incubation. It was only PaO1 and not DK2 that managed to pass through the membrane, which is probably due the high motility of PaO1.

With the single membrane setups it was thus concluded that the YPI molecule from *P. aeruginosa* passes the 220 and 450 nm Millipore membranes, but are unable to pass the nanoporous membranes. Therefore a milli-milli double membrane setup was used in an attempt to identify the YPI molecule.

It is believed that the YPI phenotype in *S. aureus* is induced by one or several quinolone molecules from *P. aeruginosa*. In the first Millipore double membrane setup experiments with *P. aeruginosa DK2 - S. aureus*, there were no sign of the YPI phenotype in *S. aureus*. This phenomenon was considered to be related to slow diffusion of signal molecules. It is possible that the difference between the signal molecule's diffusion constant in water and in LB 2% agar is too big and that the molecules therefore can go from agar to water but not the other way. In an attempt to decrease this difference, the LB 2% agar was replaced by semi-solid LB 0.5% agar. This worked as expected and the YPI phenotype was now observed in the *S. aureus* colonies in the milli-milli double membrane setup, see Figure 31A.

As mentioned above, the YPI molecule is believed to be hydrophobic and might be secreted in vesicles, which explains why the yellow pigment only is detected when the Millipore membranes, with a larger pore size than the nanoporous membranes, are used. In a previous study by Reen et al. (2) it was suggested that the *P. aeruginosa* quinolone HHQ, can induce yellow pigment production in *S. aureus*. HHQ is a hydrophobic signal molecule, which can be secreted in vesicles, and is expressed in excess by *P. aeruginosa* DK2 due to the *lasR* mutation (4). We therefore hypothesize that HHQ is a candidate for the YPI molecule from *P. aeruginosa*.

To investigate the hypothesis two HHQ-specific experiments were executed. First, *S. aureus* was spotted in petri dishes with LB 2% agar. In one petri dish, wells were formed in the agar just next to the colonies and filled with a solution of HHQ. The

HHQ would then be able to diffuse in the agar and affect the pigment production in the *S. aureus* colony. In the other petri dish, filter papers soaked in HHQ solution were placed just next to the cultures. The HHQ solutions had a concentration of 10 or 100 μM and were diluted from a 50 mM methanol stock solution (from Sigma Aldrich). After three days of incubation there was no sign of yellow pigmentation in any of the *S. aureus* colonies (data not shown). In the second experiment, *S. aureus* was cultured in petri dishes where the growth medium, 0.3% TSA, had been prepared with 10 μM HHQ solution. As in the first experiment, *S. aureus* showed no signs of induced yellow pigmentation (data not shown). Since *S. aureus* was unaffected after growth with any of the HHQ solutions, the theory about HHQ being secreted in vesicles, which may facilitate the diffusion of HHQ to the environment, was strengthened. *S. aureus* might not be able to take up single HHQ molecules from a solution, which could explain the negative result in observing the YPI phenotype in *S. aureus* from these HHQ experiments.

5.3.3 Identification of molecules in the water phases

The molecules that were found to be of interest as candidates responsible for the YPI phenotype in *S. aureus* are the quinolones with an *m/z* of 244 and 270, since they were present in two water phases where the YPI phenotype was observed. Considering that the pure solution of HHQ present in the growth medium was unable to induce the YPI phenotype in *S. aureus*, our study supports the theory that the hydrophobic nature of HHQ gives it a low solubility in water and therefore needs the presence of biosurfactants as rhamnolipids to diffuse in the growth medium. Further studies on HHQ as signalling molecule responsible for the YPI phenotype could therefore be performed with vesicle forming rhamnolipids together with HHQ in the water phase.

Since the GZI phenotype in *P. aeruginosa* DK2 was not observed in our setup, we have no suggestions for what molecule that is responsible for its appearance. Membranes with bigger pores than 450 nm should not be used in order to be sure that the bacteria cannot go through, and therefore it is unlikely that the GZI phenotype will be observed in the membrane box setup, even if the membrane parameters are changed.

5.3.3.1 MALDI-TOF MS

The *P. aeruginosa* signalling molecule HHQ, which is produced in excess in the *lasR* mutant was considered as a strong potential candidate as the YPI molecule. However it could not be confirmed, and from the MALDI-TOF MS analysis the peak at *m/z* 270 was represented to the same extent as the HHQ peak at *m/z* 244. The peak at *m/z* 270 has been reported to be the HHQ related AHQ 2-(1-nonenyl)-4(1H)-quinolone (NEHQ) (55) and in the article by Diggle et al. (55) it is shown from MS/MS analysis that both HHQ and NEHQ have a daughter ion at *m/z* 172. The peak at *m/z* 172 is present in our spectra, however it is also represented in the spectrum from the α-CHCA matrix and can therefore not be determined to be an HAQ derivate. There were several peaks in the MALDI-TOF MS spectrum from the *P. aeruginosa* PaO1 – *S. aureus* interaction that were identified as *P. aeruginosa* quinolones. Although it is known that PaO1 produces several more virulence factors and HAQ molecules compared to the CF adapted *P. aeruginosa* (15), which explains the presence of additional and more prominent peaks in the PaO1 spectrum.

The peak at *m/z* 235 was observed in all three MALDI-TOF MS spectra (Figure 33-35), but also in the *P. aeruginosa* Tn1E8 agar extract (Table 6) that was used as reference. This molecule is therefore believed to originate from *S. aureus*, which was present in all setups from where the samples were taken.

The discussed peaks in the samples from the Millipore 220 and 450 nm setup with *P. aeruginosa* DK2 (Figures 32 and 33) were not detectable when a low laser power was used for the analysis. It had to be increased to enable their detection. The increase in laser power also resulted in a periodic noise with a frequency of *m/z* 1. Some of the discussed peaks of interest were co-located with peaks from the periodic noise. However, their higher intensity makes us believe that these peaks indicate the presence of signal molecules in the samples. It was observed that the mentioned peaks in the spectra of Millipore 220 and 450 nm do not correlate. This could be explained by the fact that there probably is a difference in concentration. A higher statistical support of the water phase analysis is needed before further conclusions can be drawn.

The fundamental theory of MALDI-TOF MS is that the matrix molecules absorb the high laser energy and when the matrix desorbs from the surface, it takes the sample molecules with it into the vacuum where the time of flight can be measured. If the sample molecules are lumped together, and not well dispersed in the matrix, they will instead be burned and destroyed by the laser energy (47). Therefore it is of great importance that the sample is well spread in the matrix, and that the matrix is a good solvent for the molecules to be detected. This theory can explain the fact that the signal intensities from the quinolone peaks were higher when the samples were mixed thoroughly with ethyl acetate and left for two hours. It is expected that the hydrophobic quinolones dissolve better in ethyl acetate than in water and therefore are detected in a higher amount. The ethyl acetate might also disrupt potential transport vesicles, releasing a higher amount of signal molecules and enabling their detection.

To improve the signal acquisition in MALDI-TOF MS, different methods were tried. In addition to increased laser power, sample up-concentration was tested. To up-concentrate the water phase samples, they were reduced to half the volumes under nitrogen gas flow for one hour. The MALDI-TOF MS analysis of these samples was very poor, with barely any signals that were distinguishable from the noise. Probably, this was caused by salts in the growth medium, which concentrations became too high when the samples were up-concentrated. With too high salt concentrations the salt intensity supresses the sample signal, resulting in no distinguishable peaks in the spectrum at all (56). It would be possible to get rid of such unwanted salts by drying the samples completely and then adding a solvent in which the salts will not be solubilized.

The fact that hydrohpobic molecules are unwilling to be in an aqueous solution as the water phase, and therefore might adsorb to the sample tube walls (made of plastic), could be a contributing reason for the low concentration of singnalling molecules detected in the water phase solutions.

The MALDI-TOF MS was from the beginning aimed for amino acid detection from *S. aureus*, therefore the matrix α-CHCA was chosen, as it has been reported to be suitable for amino acid detection (53). It is possible that another matrix, more suitable

for quinolone detection, could have improved the results in the search for YPI molecules from *P. aeruginosa*.

5.3.3.2 Water phase analysis improvements

The MALDI-TOF MS analysis enabled detection of several *m/z* peaks corresponding to known *P. aeruginosa* quinolones in the water phase. As discussed, this analysis method can be improved in several ways, for example by exchanging the matrix and adjusting the laser power. MALDI-TOF MS has a high potential for the analysis of the water phases and our suggestion is that more sample preparation and optimization should be performed, in order to take advantage of this powerful instrument. Moreover, tandem mass spectroscopy (MS/MS) could be considered when the experiment has reached a certain level of knowledge of potential GZI and YPI candidates. In MS/MS, no matrix is required and its interfering background will be avoided, which is preferred. MS/MS has been used to identify molecules as quinolones (55), (57), with which the results could be compared.

MALDI-TOF MS and MS/MS analysis can, however, only provide information of what molecules that are present in the water phase, and thereby indicate potential molecules to proceed with in the detection analysis. Neither of the two methods can be used to determine the specific signal molecule responsible for the YPI phenotype. The double membrane setup could here be used to evaluate if a pure molecule solution that is introduced in the water phase can induce the YPI phenotype without the presence of *P. aeruginosa* (as tried with Casamino acid solution and *P. aeruginosa* in the nano-nano double membrane setup). Another possible way to take advantage of the water phase setup would be to introduce molecules that trap or break down the suspected signal molecules (e.g. nucleases in the case where DNA is found as signal molecule), in order to see if the GZI or YPI phenotype disappears.

5.3.3.3 UV-Vis

UV-Vis analysis of the water phases was intended to be used as an additional method for detection of the YPI and GZI molecules. The low concentration of bacterial molecules in the samples and the dominant UV-absorption of the growth medium, made it difficult. The spectra from pure Casamino acids (2%) and the 100 μM HHQ solution were added for comparison, although their signals were covered by the growth medium spectrum. Regardless of the different bacterial strains used in the double membrane setup, all water phase samples showed the same absorption spectra in the UV-Vis as the growth medium background. We could conclude that if the YPI and GZI molecules were present they would not be distinguishable from the growth medium (Figure 32). The sole spectrum to differ from the others was the water phase from *S. aureus* JE2 – PaO1, which had two absorbance peaks not visible elsewhere. These peaks indicated the presence of the green pigment pyocyanin (54) that is typical for *P. aeruginosa* PaO1. As the PaO1 sample was colored slightly green this was expected.

Concerning the water phase analysis, it can be concluded that with the UV-Vis method used in this study, it is not likely that any specific signalling molecules can be distinguished from the water phases.

5.4 Future prospects

In order to avoid the time consuming mounting of membranes in the setup and the potential stress from the Sugru clay, we propose to construct a two-segment device, see Figure 35A. Each segment should have an open end with an O-ring. The membrane would then be clamped between the O-rings of the two segments, and easy to exchange. This would make the method easier to standardize with respect to the membrane dimensions. On the other hand it would demand a more complex construction with three segments for the double membrane setup, see Figure 35B. The middle segment, containing the water phase, would then require being completely tight to avoid leakage. Another important improvement is to construct a lid for the midsection of the double membrane setup to minimize evaporation of the water phase.

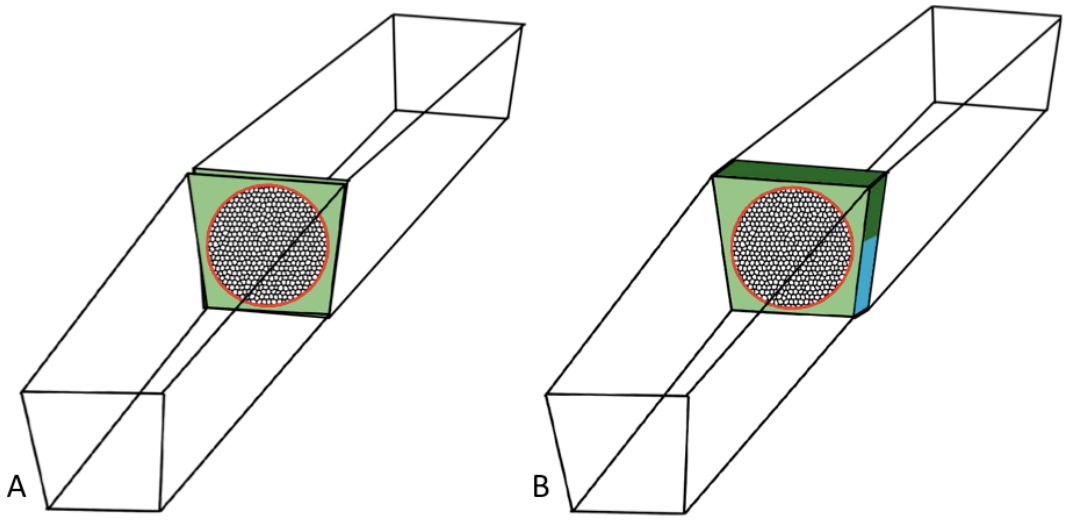

Figure 36: The proposed future construction of A) the single membrane setup, and B) the double membrane setup with a water phase.

In order to succeed in the analysis of bacterial interaction in the proposed setup, we recommend consideration of the following parameters:

- **Choice of growth medium.** The medium should enhance the expression of the bacterial phenotype, to facilitate its observation.
- **Membrane characteristics.** The membranes should be of different kinds to enable the characterization of signal molecules based on for example pore size and hydrophilicity. A variety of membranes make it easier to circle the signal molecules of interest. Other important membrane parameters are biocompatibility, thickness, homogeneity and pore distribution, the consistency in membrane production is therefore of high importance.
- **Water phase analysis method.** We propose the usage of analysis techniques which only requires small amounts of samples, and which can detect compounds at low concentrations.
    - If MALDI-TOF MS is used the matrix and instrument settings should be adapted for detection of the possible signal molecules. Additionally, sample up-concentration should be considered.
    - Mass spectroscopy (MS/MS) was not performed in this study. However, it is considered as an alternative method for signal molecule detection.

6 Conclusion

We have realized a new type of growth chamber for studies of bacterial interspecies communication, which could be a key in the development of new effective therapies against polymicrobial infections in humans. By using commercially available Millipore membranes with a pore size of 220 and 450 nm respectively, we showed that the bacteria *S. aureus* and *P. aeruginosa* can perform cell-cell communication through a membrane. In addition it was concluded that the bacteria have the potential to affect each other when separated by a water phase. The water phase was analyzed and the presence of several *P. aeruginosa* specific quinolones was confirmed.

This is of high interest in the search for the specific signal molecules that *S. aureus* and *P. aeruginosa* exchange. The aim was to characterize the yellow pigment inducing (YPI) molecule from *P. aeruginosa* and the growth zone inducing (GZI) molecule from *S. aureus*. We had an initial hypothesis of amino acids from *S. aureus* inducing the growth zone in *P. aeruginosa* and HHQ from *P. aeruginosa* inducing the yellow pigment production in *S. aureus*, however, further studies are needed to confirm or reject this. Notably, we did detect HHQ in the water phase from which we observed the YPI phenotype in *S. aureus*.

The production of hydrophilic nanoporous membranes was successful, which was confirmed by various characterization methods. The production can be further refined to achieve more homogenous membranes and enable customization of for example thickness and hydrophilicity. However the pore size of 10 nm seemed to be too small for the passage of the YPI molecule and the GZI molecule from *P. aeruginosa* and *S. aureus* respectively, and therefore the YPI and GZI phenotypes were not observed in this setup.

7 References

1. **Tashiro Y, Yawata Y, Toyofuku M, Uchiyama H, Nomura N.** Interspecies Interaction between *Pseudomonas aeruginosa* and Other Microorganisms. *Microbes Environ*. 2013, Vol. 28:13–24, DOI: 10.1264/jsme2.ME12167.

2. **Reen F J, Mooij M J, Holcombe L J, McSweeney C M, McGlacken G P, Morrissey J P, O'Gara F.** The Pseudomonas quinolone signal (PQS), and its precursor HHQ, modulate interspecies and interkingdombehaviour. *FEMS Microbioloy Ecology*. 2011, Vol. 77:413–428, DOI: 10.1111/j.1574-6941.2011.01121.x.

3. **Camilli A, Bassler B L.** Bacterial Small-Molecule Signaling Pathway. *Sciene*. 2006, Vol. 311:1113-1116, DOI: 10.1126/science.1121357.

4. **Michelsen C F, Christensen AM J, Bojer M S, Høiby N, Ingmer H, Jelsbak L.** *Staphylococcus aureus* Alters Growth Activity, Autolysis, and Antibiotic Tolerance in a Human Host-Adapted Pseudomonas aeruginosa Lineage. *Journal of Bacteriology*. 2014, Vol. 196:3903–3911, DOI: 10.1128/JB.02006-14.

5. **Mulder M.** *Basic principles of membrane technology* . Netherlands : Kluwic academic publisher, 1996. ISBN: 0-7923-4247-X.

6. **Cui Z F, Jiang Y, Field R W.** Fundamentals of Pressure-Driven Membrane Separation Processes. *Membrane technology*. 2010, DOI: 10.1016/B978-1-85617-632-3.00001-X.

7. **Li L.** *Nanoporous polymers for membrane applications*. Copenhagen : J&R Frydenberg A/S, 2012. ISBN: 978-87-92481-61-0.

8. **Schulte L, Grydgaard A, Jakobsen M R, Szewczykowski P P, Guo F , Vigild M E , Berg R H, Ndoni S.** Nanoporous materials from stable and metastable structures of 1,2-PB-b-PDMS block copolymers. *Polymer*. 2011, Vol. 52:422-429, DOI: 10.1016/j.polymer.2010.11.038.

9. **Guo F, Jankova K, Schulte L, Vigild ME, Ndoni S.** Surface Modification of Nanoporous 1,2-Polybutadiene by Atom Transfer Radical Polymerization or Click Chemistry. *Langmuir*. 2010, Vol. 26:2008-2013, DOI: 10.1021/la9025443.

10. **Merck KGaA.** Merck Millipore. *GVWP02500 | Durapore Membrane Filter, PVDF, Hydrophilic, 0.22 µm, 25 mm, white, plain*. [Online] Merck Millipore Corporation, 2015. [Retrived: 26 May 2015.] http://www.merckmillipore.com/SE/en/product/Durapore-Membrane-Filter%2C-PVDF%2C-Hydrophilic%2C-0.22%C2%A0%C2%B5m%2C-25%C2%A0mm%2C-white%2C-plain,MM_NF-GVWP02500?CategoryName=0000000a00016e9000040023&&CategoryDomainName=Merck-MerckMillipore#anchor_Descript.

11. **Ryan R P, Dow J M.** Diffusible signals and interspecies communication in bacteria. 2008, Vol. 154: 1845-1858, DOI: 10.1099/mic.0.2008/017871-0.

12. **Hoffman L R, Déziel E, D'Argenio D A, Lépine F, Emerson J, McNamara S, Gibson R L, Ramsey B W, Miller S I.** Selection for *Staphylococcus aureus* small-colony variants due to growth in the presence of Pseudomonas aeruginosa. *PNAS*. 2006, Vol. 103:19890–19895, DOI: 10.1073/pnas.0606756104.

13. **Folkesson A, Jelsbak L, Yang L, Johansen H K , Ciofu O, Høiby N, Molin S.** Adaptation of *Pseudomonas aeruginos*a to the cystic fibrosis airway: an evolutionary perspective. *NATURE REVIEWS | MICROBIOLOGY*. 2012, Vol. 10:841-851, DOI: 10.1038/nrmicro2907, ss. 841-851.

14. **Palmer K L, Mashburn L M, Singh P K, Whiteley M.** Cystic Fibrosis Sputum Supports Growth and Cues Key Aspects of *Pseudomonas aeruginosa* Physiology. *Journal of Bacteriology*. 2005, Vol. 187:5267–527, DOI: 10.1128/JB.187.15.5267–5277.2005.

15. **D'Argenio D A, Wu, M, Hoffman, L R, Kulsekara H D, Déziel E, Smith E E, Nguyen H et. al.** Growth phenotypes pf *Pseudomonas aeruginosa lasR* mutants adapted to the airways of cystic fibrosis patients. *Molecular Microbiology*. 2007, Vol. 64:512-533, DOI: 10.1111/j.1365-2958.2007.05678.x.

16. **Korgaonkar A, Trivedib U, Rumbaughb K P, Whiteley M.** Community surveillance enhances *Pseudomonas aeruginosa* virulence during polymicrobial infection. *PNAS*. 2013, Vol. 110:1059–1064, DOI: 10.1073/pnas.1214550110.

17. **Lazzari M, Liu G, Lecommandoux S.** *Block Copolymers in Nanoscience*. Weinheim : WILEY-VCH Verlag GmbH & Co. KGaA, 2006. ISBN: 978-3-527-31309-9.

18. **Hamley I W, Koppi K A, Rosedale J H, Bates F S, Almdal K, Mortensen K.** Hexagonal mesophases between lamellae and cylinders in a diblock copolymer melt. *Macromolecules*. 1993, Vol. 26:5959-5970.

19. **materials, The research group: Self-organized nanoporous.** Unpublished results. u.o. : DTU Nanotech, 2013.

20. **Hsieh H, Quirk R P.** *Anionic Polymerization: Principles and Practical Applications* . New York : Marcel Dekker, 1996. ISBN: 0-8247-9523-7.

21. **Roberts J D, Caserio M C.** *Basic Principles of Organic Chemistry, sec. ed. .* Menlo Park, CA. : W. A. Benjamin, Inc., 1977. ISBN: 0-8053-8329-8.

22. **Morton M.** *Anionic Polymerization: Principles and Practice*. New York : Academic Press, 1983.

23. **Fengxiao G.** *Functional Nanoporous Polymers from Block Copolymer Precursors*. Copenhagen : J&R Frydenberg A/S, 2012. ISBN: 978-87-92481-25-2.

24. **Li L, Schulte L, Clausen L D, Hansen K M, Jonsson G E.** Gyroid Nanoporous Membranes with Tunable Permeability. *ACS Nano*. 2011, Vol. 5:7754–7766, DOI: 10.1021/nn200610r.

25. **Arkema.** Arkema Inc. [Online] 2007. [Retrived: 6 May 2015.] www.luperox.com.

26. **Corey E J, Venkateswarlu A.** Protection of hydroxyl groups as tert-butyldimethylsilyl derivatives. *J. Am. Chem. Soc*. 1972, Vol. 94:6190-6191, DOI: 10.1021/ja00772a043.

27. **Berthold A, Sagar K, Ndoni S.** Patterned Hydrophilization of Nanoporous 1,2-PB by Thiol-ene Photochemistry. *Macromolecular Rapid Communications*. 2011, Vol. 32:1259–1263, DOI: 10.1002/marc.201100243.

28. **Porex Corporation.** Porex - Advanced Porous Materials. [Online] 2015. [Retrived: 27 May 2015.] http://www.porex.com/technologies/materials/porous-plastics/polyvinylidene-fluoride/.

29. **Pall Corporation.** PALL. [Online] 2015. [Retrieved: 27 May 2015.] http://www.pall.com/main/oem-materials-and-devices/product.page?id=47593.

30. **Levison M E.** Merck manual. *Merck Sharp & Dohme Corp*. [Online] 2015. [Retrived: 4 May 2015.] http://www.merckmanuals.com/home/infections/bacterial-infections/i-staphylococcus-aureus-i-infections.

31. **Plata K, Rosato A E, Węgrzyn G.** *Staphylococcus aureus* as an infectious agent: overview of biochemistry and molecular genetics of its pathogenicity. *Acta Biochimica Polonica*. 56:597–612, 2009.

32. **Franklin D L.** *Staphylococcus aureus* infections. *The New England Journal of Medicine*. p. 520-532, 1998.

33. **Antonic V, Stojadinoic, A, Zhang B, Izadjoo M J, Alavi M.** *Pseudomonas aeruginosa* induces pigment production and enhances virluence in a white phenotypic variant of *Staphylococcus aureus*. *Dovepress*. 2013, Vol. 6:175-186, DOI: 10.2147/IDR.S49039.

34. **Pier G B, Lyczak J B, Wetzler L M.** *Immunology, Infection, and Immunity*. Washington : ASM Press, 2004. ISBN: 978-1555812461.

35. **Farrow III J M, Pesci E C.** Two Distinct Pathways Supply Anthranilate as a Precursor of the Pseudomonas Quinolone Signal. *Journal of bacteriology*. 2007, Vol. 189:3425–3433, DOI: 10.1128/JB.00209-07.

36. **Michelsen C F, Khademi S M H, Johansen H K, Ingmer H, Dorrestein P C, Jelsbak L.** Evolution of metabolic divergence in *Pseudomonas aeruginosa* facilitates a mutualistic interspecies interaction. 2015.

37. **Zhou L, Reen F J, O'Gara F, McSweeney C M, Clarke S L, Glennon J D, Luong J H T, McGlacken G P.** Analysis of pseudomonas quinolone signal and other bacterial signalling molecules using capillaries coated with highly charged polyelectrolyte monolayers and boron doped diamond electrode. *Journal of Chromatography A*. 2012, Vol. 1251:169– 175, DOI: 10.1016/j.chroma.2012.06.064.

38. **Diggle S P, Cornelis P, Williams P, Cámara M.** 4-Quinolone signalling in *Pseudomonas aeruginosa*: Old molecules, new perspectives. *International Journal of Medical Microbiology*. 2006, Vol. 296:83-91, DOI: 10.1016/j.ijmm.2006.01.038.

39. **Mashburn-Warren L, Howe J, Brandenburg K, Marvin Whiteley M.** Structural Requirements of the Pseudomonas Quinolone Signal for Membrane Vesicle Stimulation. *Journal of Bacterology*. 2009, Vol. 191:3411–3414, DOI: 10.1128/JB.00052-09.

40. **Marvig R L, Johansen H K, Molin S, Jelsbak L.** Genome Analysis of a Transmissible Lineage of *Pseudomonas aeruginosa* Reveals Pathoadaptive Mutations and Distinct Evolutionary Paths of Hypermutators. *PLOS Genetics*. 2013, Vol. 9:e1003741, DOI: 10.1371/journal.pgen.1003741.

41. **Optics, Philips Electron.** *Environmental Scanning Electron Micrscopy - An Introduction to ESEM*. Netherlands: Eindhoven : Robert Johnson Associates, 1996.

42. **Williams D B, Barry C C.** *Transmission Electron Microscopy: A textbook for material science*. . : Springer US, 2009. ISBN: 978-0-387-76500-6.

43. **Griffiths P, de Hasseth J A.** *Fourier Transform Infrared Spectrometry (2nd ed.)*. u.o. : Wiley-Blackwell, 2007. ISBN: 0-471-19404-2.

44. **Sciences, Perkin Elmer Life and Analytical.** *FT-IR Spectroscopy—Attenuated Total Reflectance (ATR)*. 2005, Retrieved: 2007-01-26.

45. **Attension.** Static and dynamic contact angles and their measurement techniques. *Attension - Biolin Scientific*. [Online] 2014. [Retrived: 5 May 2015.] http://www.biolinscientific.com/zafepress.php?url=%2Fpdf%2FAttension%2FTheory%20Notes%2FAT_TN_1_contactangle.pdf.

46. **Schmid F X.** Biological Macromolecules: UV-visible Spectrophotometry. *Encyclopedia of life science*. 2001.

47. **Marvin L F, Roberts M A, Fay L B.** Matrix-assisted laser desorption/ionization time-of-flight mass spectrometry in clinical chemistry. *Clinica Chimica Acta*. 2003, Vol. 337:11-21, DOI: 10.1016/j.cccn.2003.08.008.

48. **Sugru, FORMEROL F.10.** MSDS Sugru. *Sugru*. [Online] 2012. [Retrived: 12 March 2015.] www.sugru.com.

49. **FormFormForm.** Sugru. [Online] 2015. [Retrived: 12 March 2015.] www.sugru.com.

50. **Scientific Polymer, Inc.** Scientific polymer. [Online] 2013. [Retrived: 28 April 2015.] http://scientificpolymer.com/density-of-polymers-by-density/.

51. **Fey PD, Endres JL, Yajjala VK, Widhelm TJ, Boissy RJ, Bose JL, Bayles KW.** A genetic resource for rapid and comprehensive phenotype screening of nonessential *Staphylococcus aureus* genes. *mBio*. 2013, Vol. 4:e00537–12, DOI: 10.1128/mBio.00537-12.

52. **Stover CK, Pham XQ, Erwin AL, Mizoguchi SD, Warrener P, Hickey MJ, Brinkman FSL, Hufnagle WO, Kowalik DJ, Lagrou M et al.** Complete genome sequence of *Pseudomonas aeruginosa* PAO1, an opportunistic pathogen. *Nature*. 2000, Vol. 406:959 –964, DOI: 10.1038/35023079.

53. **Gogichaeva N V, Michail A A.** Amino Acid Analysis by Means of MALDI TOF Mass Spectrometry or MALDI TOF/TOF Tandem Mass Spectrometry. [bokförf.] Hunziker P Michail A A. *Amino Acid Analysis: Methods and Protocols, Methods in Molecular Biology*. u.o. : Springer Protocols. ISBN: 978-1-61779-444-5, 2012, Vol. 828.

54. **Mavrodi D V, Bonsall R F, Delaney S M, Soule M J, Phillips G, Thomashow L S.** Functional Analysis of Genes for Biosynthesis of Pyocyanin and Phenazine-1-Carboxamide from *Pseudomonas aeruginosa* PAO1. *Journal of bacteriology*. 2001, Vol. 183:6454–6465, DOI: 10.1128/JB.183.21.6454–6465.2001.

55. **Diggle S P, Lumjiaktase P, Dipilato, Winzer K, Dipilato F, Winzer K, Chhabra S R, Ca´mara M, Williams P.** Functional Genetic Analysis Reveals a 2-Alkyl-4-Quinolone Signaling System in the Human Pathogen Burkholderia pseudomallei and Related Bacteria. *Chemistry & Biology*. 2006, Vol. 13:701–710, DOI: 10.1016/j.chembiol.2006.05.006.

56. **Iowa State University of Science and Technology.** MALDI-TOF Mass Analysis. *The Protein Facility of the Iowa State University Office of Biotechnology*. [Online] 2015. [Retrived: 24 May 2015.] http://www.protein.iastate.edu/maldi.html.

57. **Watrous J, Roach P, Alexandrov T, Heath B S, Yang J Y, Kersten R D, van der Voort M, Pogliano K, Gross H, Raaijmakers J M, Moore B S, Laskin J, Bandeira N, Dorrestein P C.** Mass spectral molecular networking of living microbial colonies. *Proc Natl Acad Sci USA*. 2012, Vol. 109:E1743-1752, DOI: 10.1073/pnas.1203689109.

58. **Mashburn L M, Whiteley M.** Membrane vesicles traffic signals and facilitate group activities in a prokaryote. *Nature*. 2005, Vol. 437:422-425, DOI: 10.1038/nature03925.

Figure 37: The phenotypes Malin and Karin cultured on LTH medium and incubated for 5 years to attain a master°.

Appendix 1 – Bacterial phenotypes

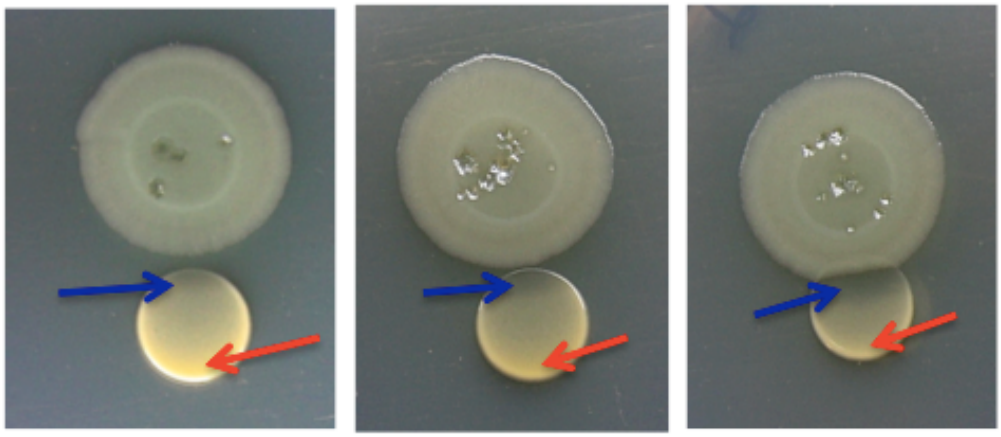

Figure 1: The interaction between *P. aeruginosa* PaO1 (above) and *S. aureus* (below) after two days of incubation. The colonies are grown at different distances from each other in the three pictures. Blue arrows indicate inhibition of *S. aureus* and red arrows indicate the YPI phenotype in *S. aureus*.

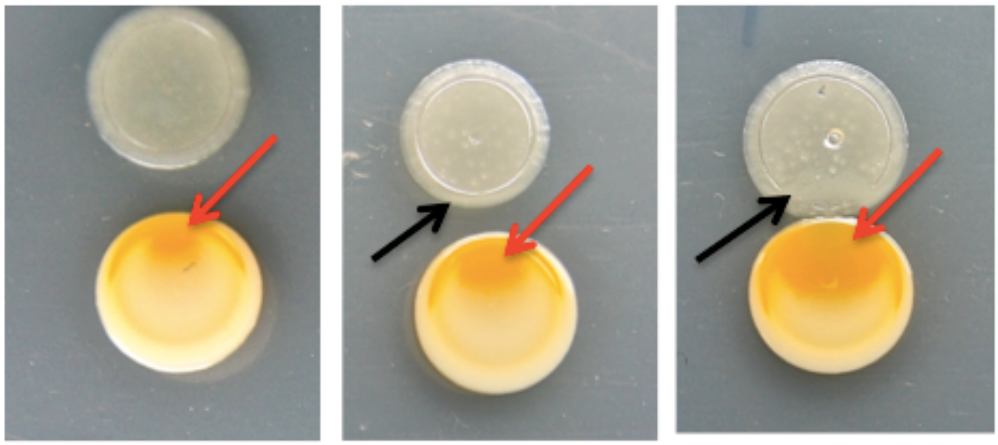

Figure 2: The interaction between *P. aeruginosa* DK2 (above) and *S. aureus* (below) after two days of incubation. The colonies are grown at different distances from each other in the three pictures. Black arrows indicate the GZI phenotype in *P. aeruginosa* DK2 and red arrows indicate the YPI phenotype in *S. aureus*.

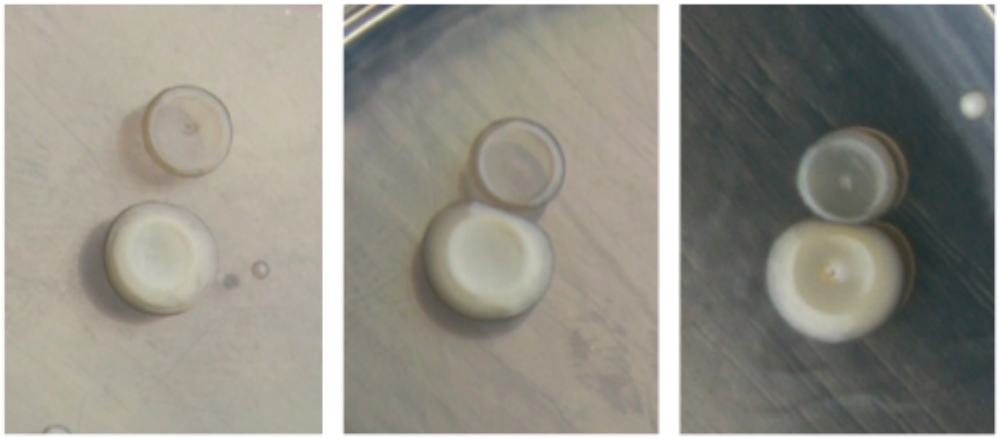

Figure 3: The interaction between *P. aeruginosa* Tn1E8 (above) and *S. aureus* (below) after two days of incubation. The colonies are grown at different distances from each other in the three pictures. No change in morphology is observed.

Appendix 2 – MALDI-TOF MS spectra

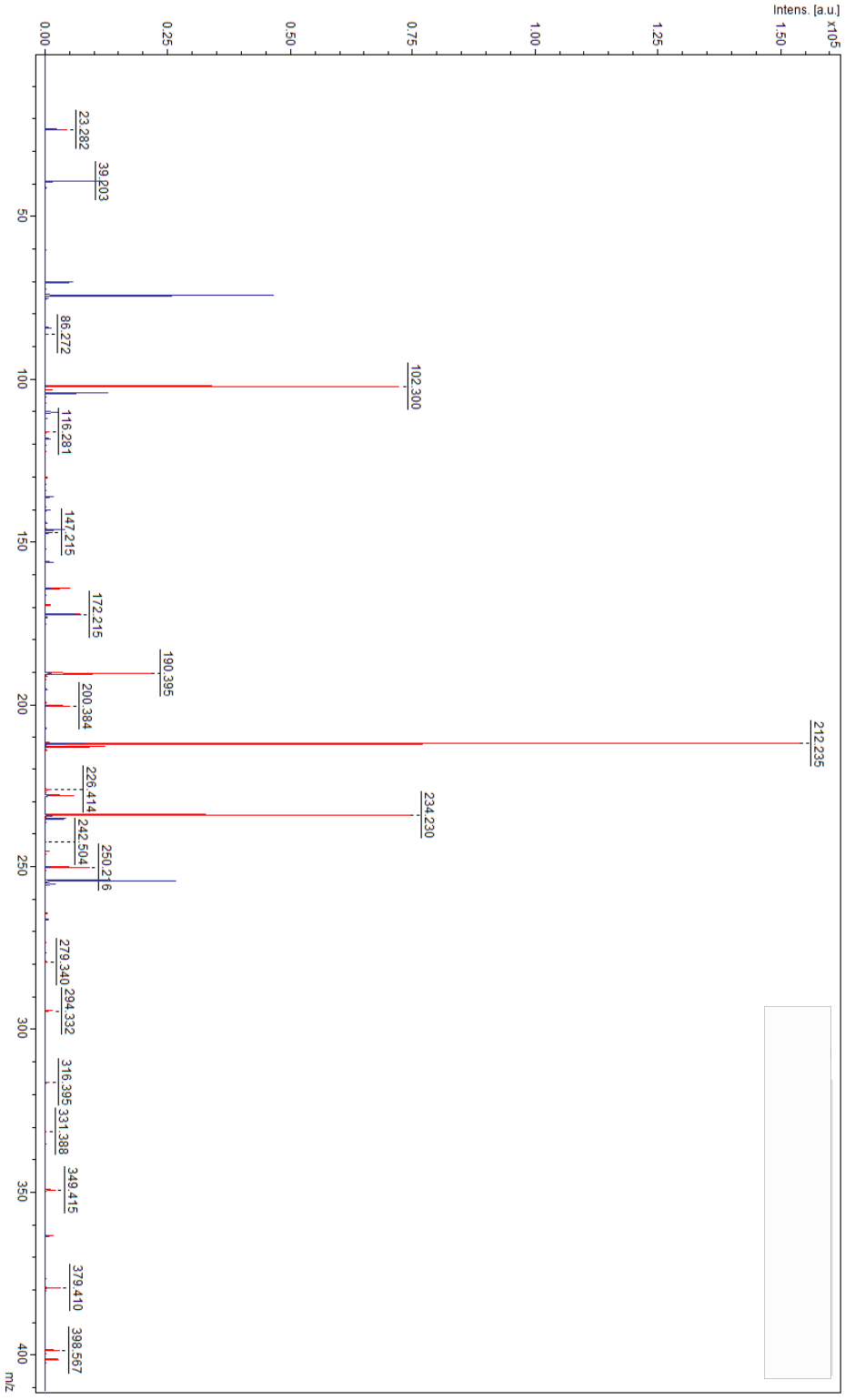

Figure 1: Water phase analysis of the *P. aeruginosa* DK2 - *S. aureus* JE2 interaction in the 220 nm Millipore double membrane setup (blue spectrum), with an agar extract from the *P. aeruginosa* Tn1E8 – *S. aureus* JE2 interaction as reference (red spectrum).

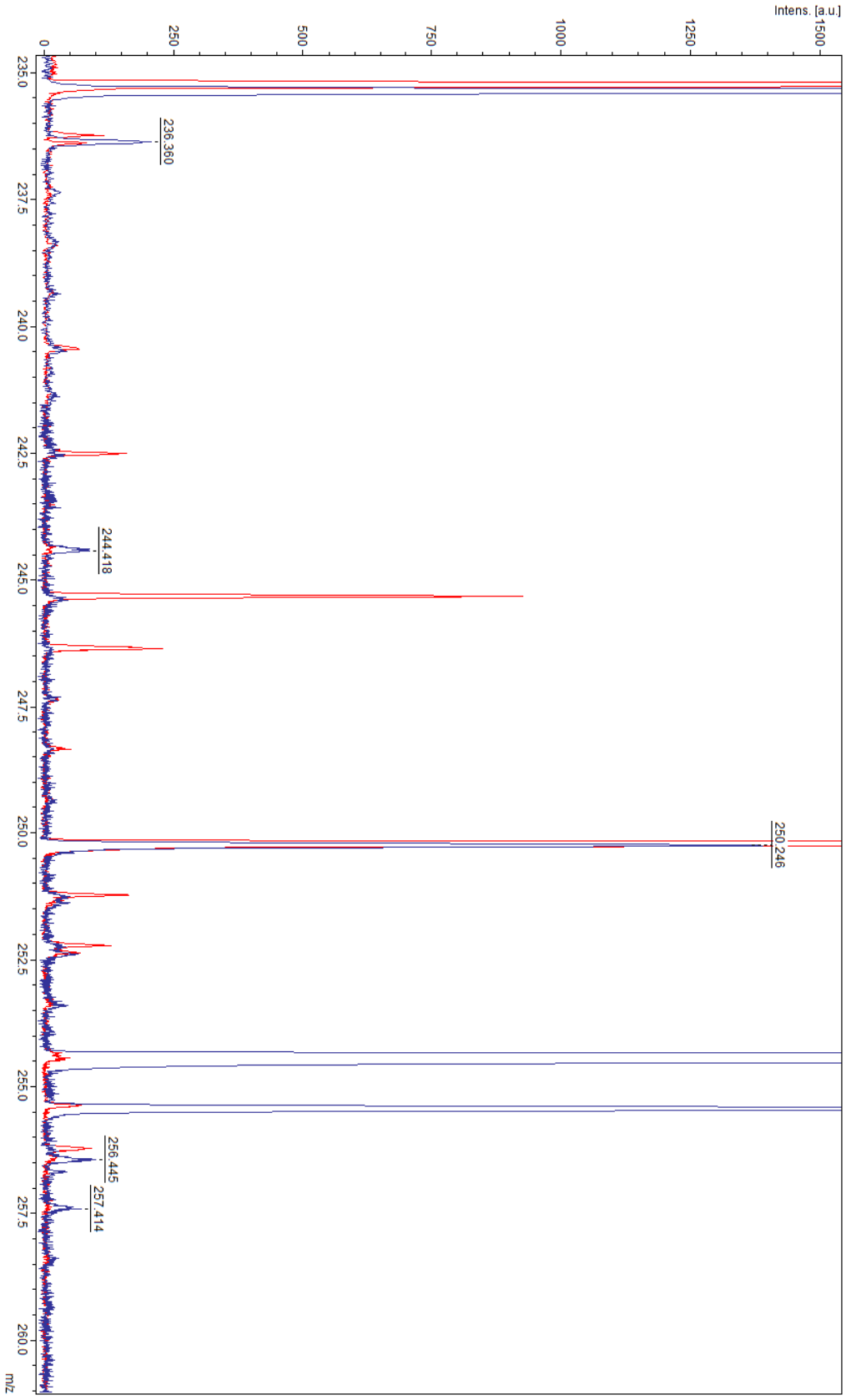

Figure 2: Close-up of spectrum in Figure 1, from *m/z* 235-250.

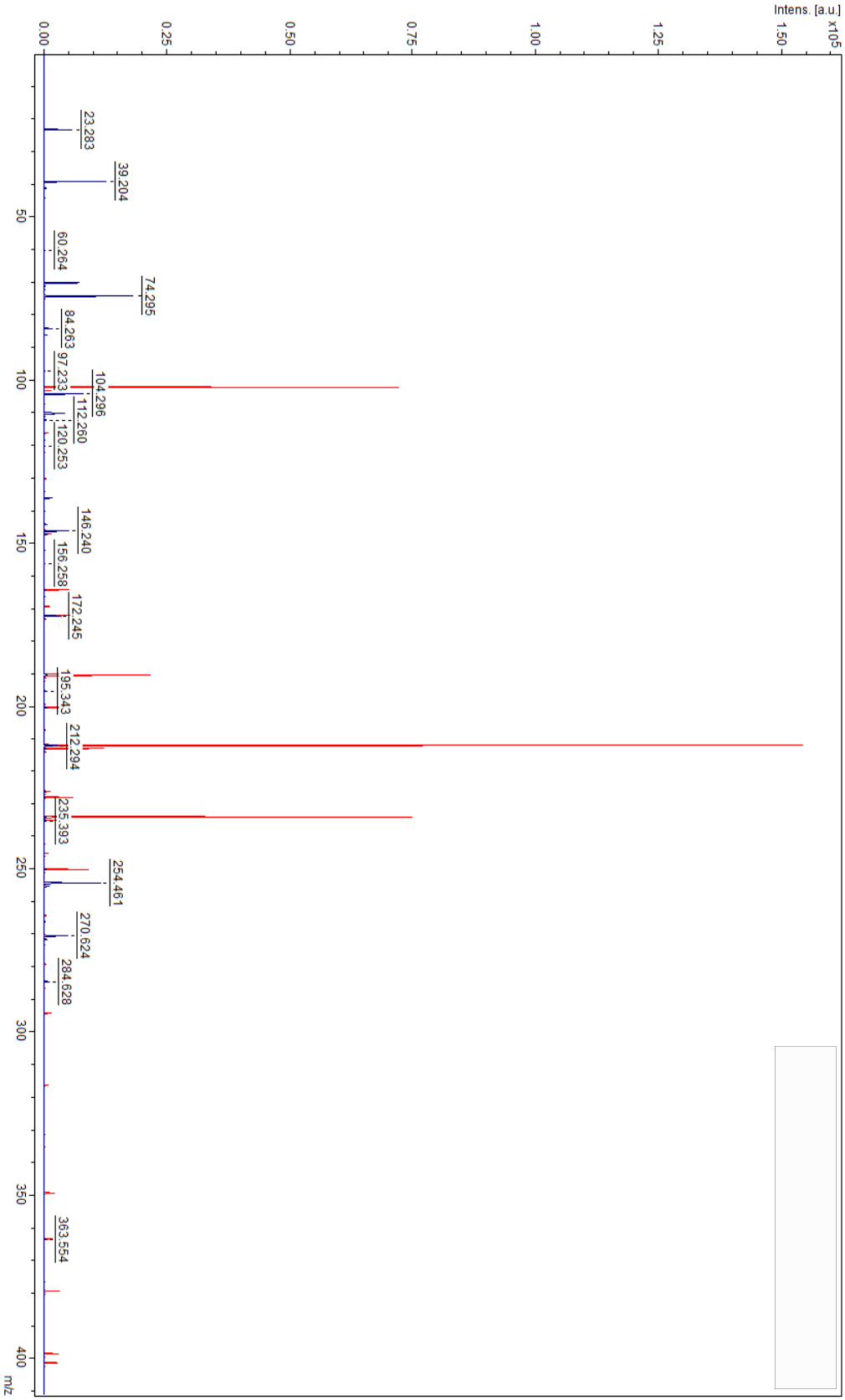

Figure 3: Water phase analysis of the *P. aeruginosa* DK2 - *S. aureus* JE2 interaction in the 450 nm Millipore double membrane setup (blue spectrum), with an agar extract from the *P. aeruginosa* Tn1E8 – *S. aureus* JE2 interaction as reference (red spectrum).

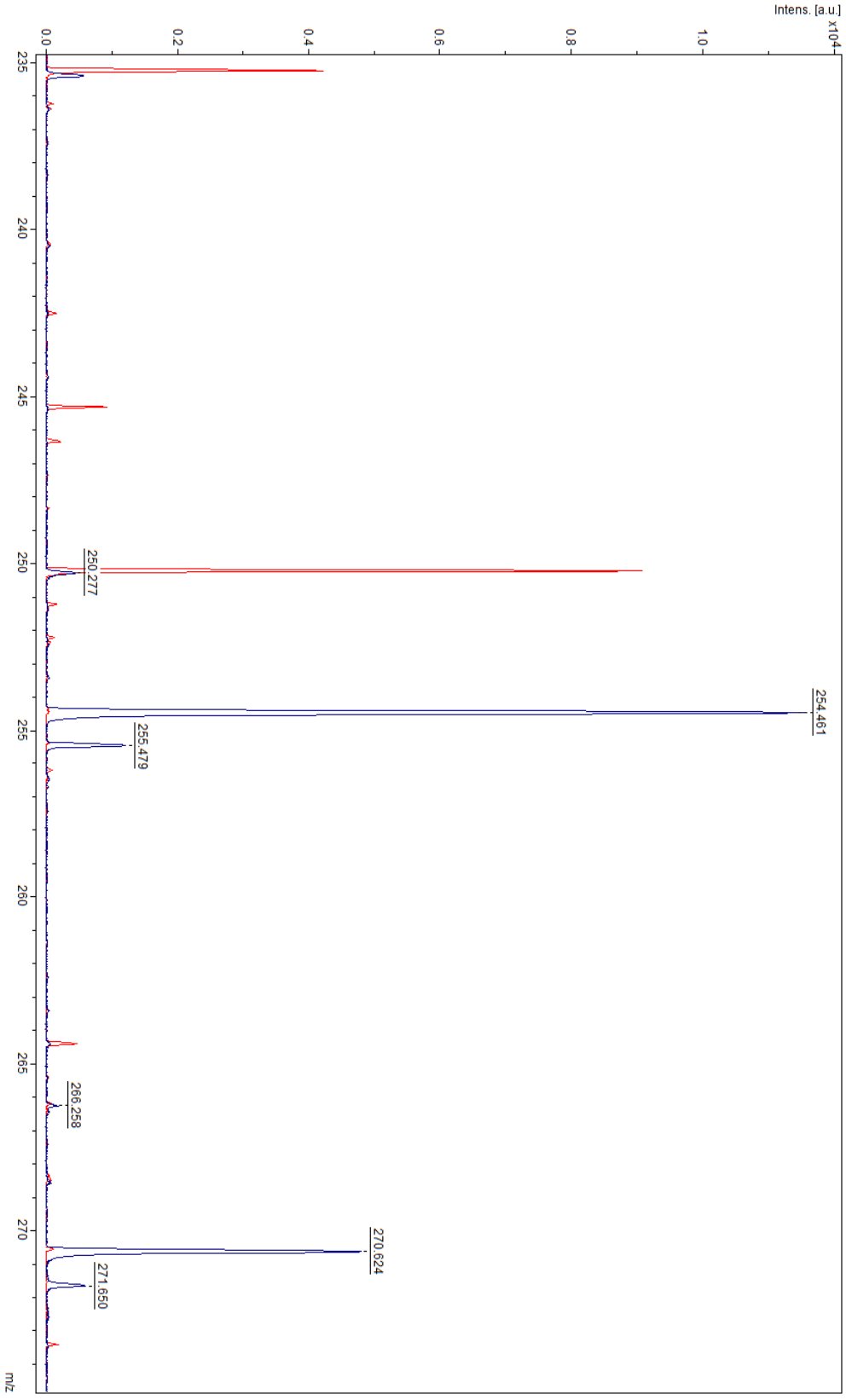

Figure 4: Close-up of spectrum in Figure 3, from *m/z* 235-280.

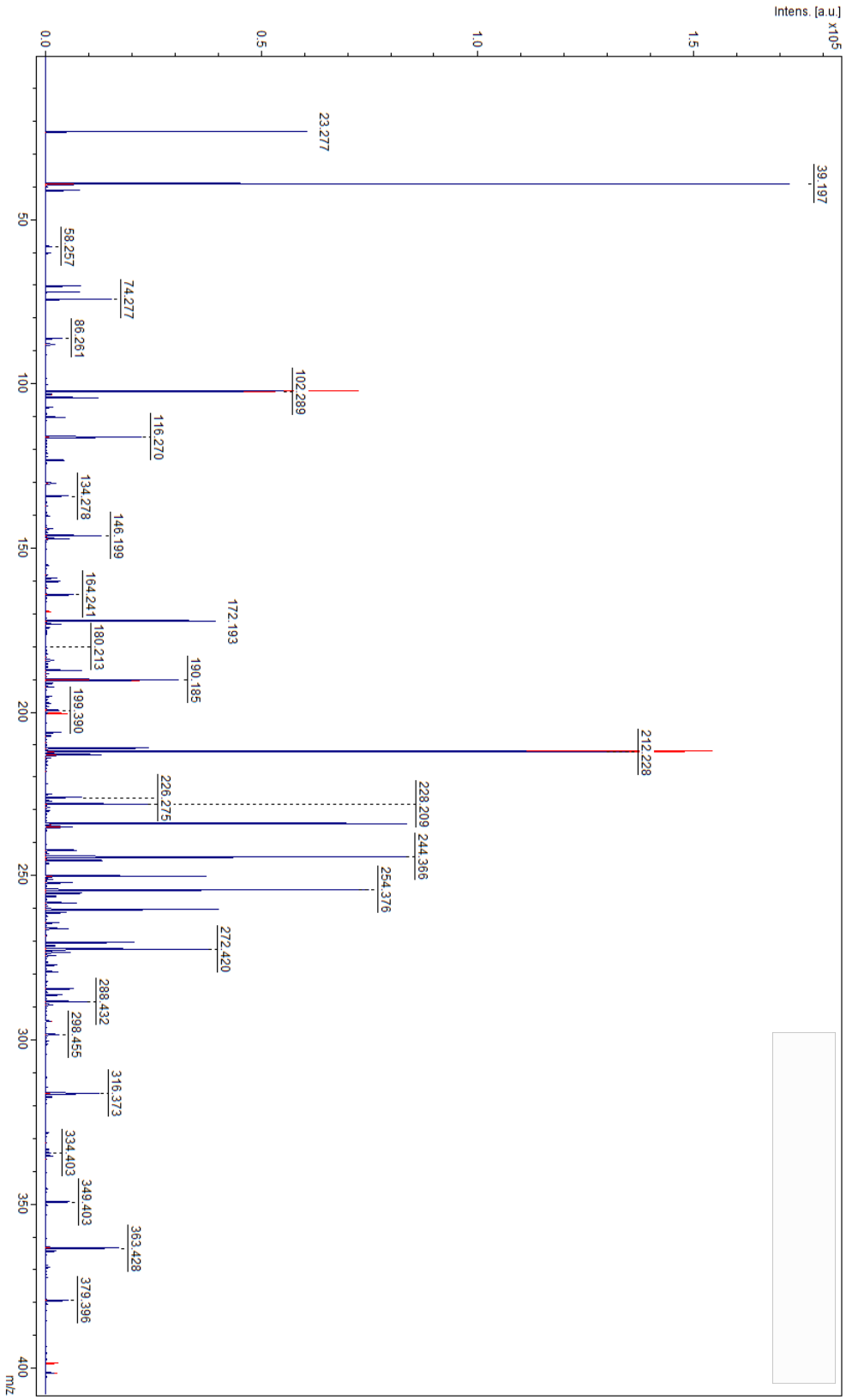

Figure 5: Water phase analysis of the *P. aeruginosa* PaO1 - S. aureus JE2 interaction in the 450 nm Millipore double membrane setup (blue spectrum), with an agar extract from the *P. aeruginosa* Tn1E8 – *S. aureus* JE2 interaction as reference (red spectrum).

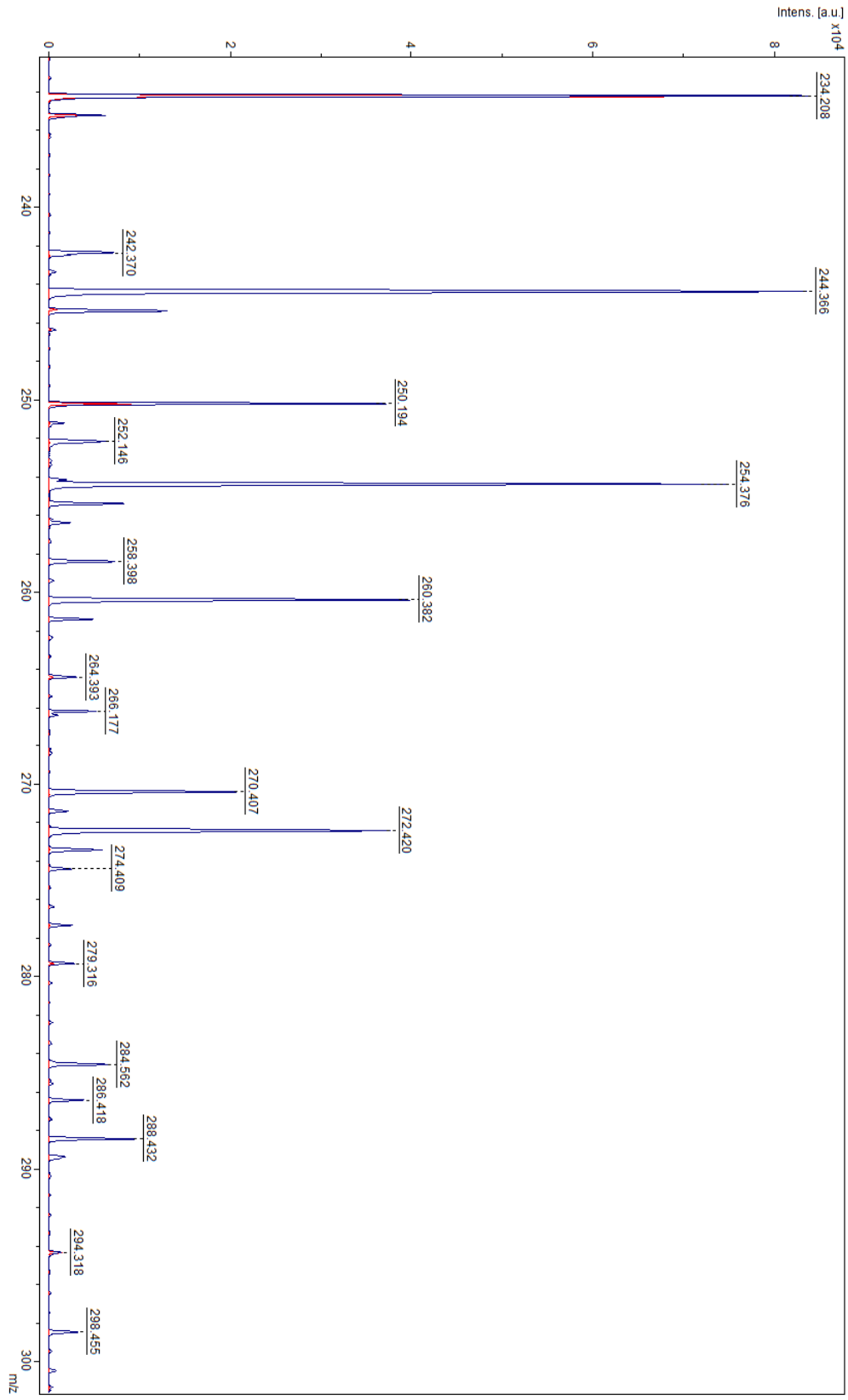

Figure 6: Close-up of spectrum in Figure 5, from *m/z* 234-300.